General Disclaimer

One or more of the Following Statements may affect this Document

- This document has been reproduced from the best copy furnished by the organizational source. It is being released in the interest of making available as much information as possible.

- This document may contain data, which exceeds the sheet parameters. It was furnished in this condition by the organizational source and is the best copy available.

- This document may contain tone-on-tone or color graphs, charts and/or pictures, which have been reproduced in black and white.

- This document is paginated as submitted by the original source.

- Portions of this document are not fully legible due to the historical nature of some of the material. However, it is the best reproduction available from the original submission.

NASA CR 168272
Contract No. NAS3-23052

PYROELECTRIC CONVERSION IN SPACE —

A CONCEPTUAL DESIGN STUDY

September 1983

Chronos Research Laboratories, Inc.

SUMMARY

Pyroelectric conversion is potentially a very lightweight means of providing electrical power generation in space. This study evaluated two conceptualized systems approaches for the direct conversion of heat (from sunlight) into electrical energy using the pyroelectric effect of a new class of polar polymers. Both of the approaches involved large area thin sheets of plastic which are thermally cycled by radiative input and output of thermal energy. The systems studied are expected to eventually achieve efficiencies of the order of 8% and may deliver as much as one half kilowatt per kilogram.

In addition to potentially very high specific power, the pyroelectric conversion approaches outlined appear to offer low cost per watt in the form of an easily deployed, flexible, strong, electrically "self-healing", and high voltage sheet.

This study assessed several potential problems such as plasma interactions and radiation degradation and suggests approaches to overcome them. The fundamental technological issues for space pyroelectric conversion are 1)demonstration of the conversion cycle with the proposed class of polymers, 2) achievement of improved dielectric strength of the material, 3) demonstration of acceptable plasma power losses for low altitude, and 4)establishment of reasonable lifetime for the pyroelectric material in the space environment. Recommendations included an experimental demonstration of the pyroelectric conversion cycle followed by studies to improve the dielectric strength of the polymer and basic studies to discover additional pyroelectric materials.

1. Report No.	2. Government Accession No.	3. Recipient's Catalog No.
NASA CR-168272		

4. Title and Subtitle	5. Report Date
PYROELECTRIC CONVERSION IN SPACE- A CONCEPTUAL DESIGN STUDY	September 1983
	6. Performing Organization Code
7. Author(s)	8. Performing Organization Report No.
R.B. Olsen	
	10. Work Unit No.
9. Performing Organization Name and Address	11. Contract or Grant No.
Chronos Research Laboratories, Inc. 3025 Via de Caballo Olivenhain, California 92024	NAS-23052
	13. Type of Report and Period Covered
12. Sponsoring Agency Name and Address	Contractor Report
National Aeronautics and Space Administration Washington, D.C. 20546	14. Sponsoring Agency Code

15. Supplementary Notes

Project Manager, Bernard L. Sater, Advanced Energetics Program, NASA Lewis Research Center, Cleveland Ohio

16. Abstract

Pyroelectric conversion is potentially a very lightweight means of providing electrical power generation in space. This study evaluated two conceptualized systems approaches for the direct conversion of heat (from sunlight) into electrical energy using the pyroelectric effect of a new class of polar polymers. Both of the approaches involved large area thin sheets of plastic which are thermally cycled by radiative input and output of thermal energy. The systems studied are expected to eventually achieve efficiencies of the order of 8% and may deliver as much as one half kilowatt per kilogram.
In addition to potentially very high specific power, the pyroelectric conversion approaches outlined appear to offer low cost per watt in the form of an easily deployed, flexible, strong, electrically "self-healing", and high voltage sheet. This study assessed several potential problems such as plasma interactions and radiation degradation and suggests approaches to overcome them. The fundamental technological issues for space pyroelectric conversion are 1) demonstration of the conversion cycle with the proposed class of polymers, 2) achievement of improved dielectric strength of the material, 3) demonstration of acceptable plasma power losses for low altitude, and 4) establishment of reasonable lifetime for the pyroelectric material in the space environment. Recommendations include an experimental demonstration of the pyroelectric conversion cycle followed by studies to improve the dielectric strength of the polymer and basic studies to discover additional pyroelectric materials.

17. Key Words (Suggested by Author(s))	18. Distribution Statement
Energy conversion Pyroelectric Power source	Unclassified - unlimited

19. Security Classif. (of this report)	20. Security Classif. (of this page)	21. No. of Pages	22. Price*
Unclassified	Unclassified	76	

*For sale by the National Technical Information Service, Springfield, Virginia 22161

FOREWORD

This final report was prepared by Chronos Research Laboratories, Inc. for NASA Lewis Research Center (LeRC) in compliance with Contract NAS3-23052.

The principal results were developed during the period of performance September 21, 1982 to September 20, 1983. A final presentation of the study results was conducted on September 20, 1983 at NASA/LeRC.

The study was conducted at Chronos by R. B. Olsen. The NASA project manager is B. L. Sater of LeRC Advanced Energetics Program.

For further information contact:

B. L. Sater
NASA/LeRC
21000 Brookpark Rd.
Cleveland, Ohio 44135
(216) 433-4000 x5221

R. B. Olsen
Chronos Research Laboratories, Inc.
3025 Via de Caballo
Olivenhain, California 92024
(619) 756-1447

ACKNOWLEDGMENTS

Chronos Research Laboratories, Inc. owes thanks to several individuals for their comments and suggestions during the preparation of this report. R.L. Anderson of American Control Engineering outlined the approach for power extraction. J.C. Hicks of the Naval Ocean System Center collaborated on the early measurements of the electrical behavior of an important copolymer. T. Mahefkey and P. Rahilly of the Aero Propulsion Laboratory at Wright-Patterson AFB, J.E. McCoy of NASA Johnson, and D. Rockey of J.P.L. were all very helpful and provided needed insight regarding the near earth space environment. Last alphabetically, but not least, special thanks go to B.L. Sater of NASA/LeRC. He first suggested the thermal storage concept described here and gave numerous quality comments during the course of this study.

TABLE OF CONTENTS

TABLE OF CONTENTS (Cont.)

LIST OF FIGURES

LIST OF TABLES

Section 1

INTRODUCTION

The pyroelectric effect is the flow of charge to and from the surfaces of a material resulting from a change in temperature (1). This effect may be used for the conversion of heat directly into electrical energy. In spite of its apparent lack of promise in the early 1960s this approach to energy conversion has been revived by recent advances. Some researchers are now suggesting that this type of conversion may be more efficient than previously believed (2), (3). In addition, in the past year, pyroelectric generators have been built which produce more than four orders of magnitude greater power than the devices of twenty years ago (4), (5), (6).

Some of the work in the early 1960s centered precisely on pyroelectric conversion in space. Experiments at NASA by Beam, Fry and Russel (7), (8) were not encouraging primarily because of 1) the particular choice of thermal-electrical cycle and 2) the lack of a pyroelectric material with high performance characteristics. In a theoretical study done by NASA in 1965 Margosian (9) summarized:

> "With currently known materials, this generator is too heavy to be of interest for electric propulsion. As a source of auxiliary power it is comparable, at best, to solar cells in weight. If materials with substantially better characteristics than those considered are found, competitive performance as a power source might be possible."

A new material has been discovered which is expected to fulfill that promise.

The purpose of the present work was to perform a conceptualized design study of a space power system utilizing such pyroelectric materials. This would permit us to establish pertinent operational characteristics and estimate performance factors on a first order basis. Also this would allow us to assess the technological barriers and potential problem areas involved with pyroelectric conversion using this film.

THEORY OF OPERATION

A pyroelectric converter is a form of heat engine which directly transforms heat energy into electrical energy. The thermodynamics of the pyroelectric converter are analogous to the more familiar steam engine with pressure-volume mechanical work replaced by voltage-charge electrical output. Before describing a pyroelectric conversion system for space power an introduction to the basic energy producing thermodynamic cycle will be helpful.

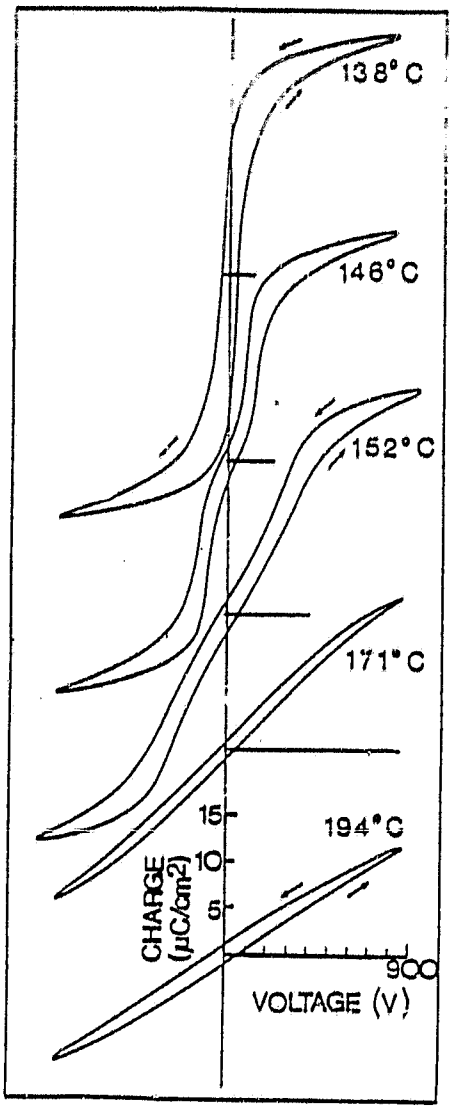

Fig. 1. Charge (Polarization) versus Applied Voltage (Electric Field) for various temperatures of 0.025cm thick $Pb_{0.99}Nb_{0.02}(Zr_{0.68}, Sn_{0.25}, Ti_{0.07})_{0.98}O_3$.

PYROELECTRIC CONVERSION CYCLE

The electrical energy production cycle may be described in terms of the charge-voltage behavior of a ferroelectric material (FE). Figure 1 illustrates, at various temperatures, the charge-voltage (polarization versus applied electric field) behavior of a ferroelectric material which may be utilized for pyroelectric conversion. Notice that the polarization is not a single valued function of the applied electric field. The polarization depends in a hysteretic way upon the applied field.

For any cyclic process an area on a charge-voltage diagram represents an electrical work since

$$W = \int V dq \qquad (1)$$

where W=electrical work, V=voltage, and q=charge. The direction of the path (clockwise or counterclockwise) determines whether electrical energy is produced or dissipated. A familiar example is the hysteretic heating of a ferroelectric element. Every time that the voltage applied to a ferroelectric sample is cycled isothermally, an amount of electrical energy (equal to the hysteresis loop area) is dissipated as heat. In this case the loop is cycled in the counterclockwise sense, as indicated by the arrows in Figure 1.

The pyroelectric generator exploits the fact that, by removing the isothermal constraint, it is possible to reverse the direction in which the loop is cycled. The loop may be cycled in a clockwise sense, thus resulting in the production of electrical energy from heat.

Shown in Figure 2 is an overlay of the charge-voltage characteristics of a ferroelectric at two different temperatures. Figure 2 also shows how clockwise cycling may be achieved when operating between these two temperatures. Starting in the upper right-hand corner at high voltage and low temperature, the FE is discharged as it is heated. After reaching a high temperature, the FE is further discharged by reducing the externally applied voltage. Thus, an electrical cycle may be executed in a clockwise manner -- opposite to the hysteretic loop direction -- in which an amount of electrical energy,

$$\int V dq = \text{Shaded area of Figure 2,} \qquad (2)$$

may be produced.

The data shown in Figures 1 and 2 correspond to measurements on a ceramic of lead zirconate modified with tin and titanium (PZST). The discovery of this material, with its unusually good pyroelectric properties, allowed the recent upsurge in the development of pyroelectric conversion (4), (5), (6).

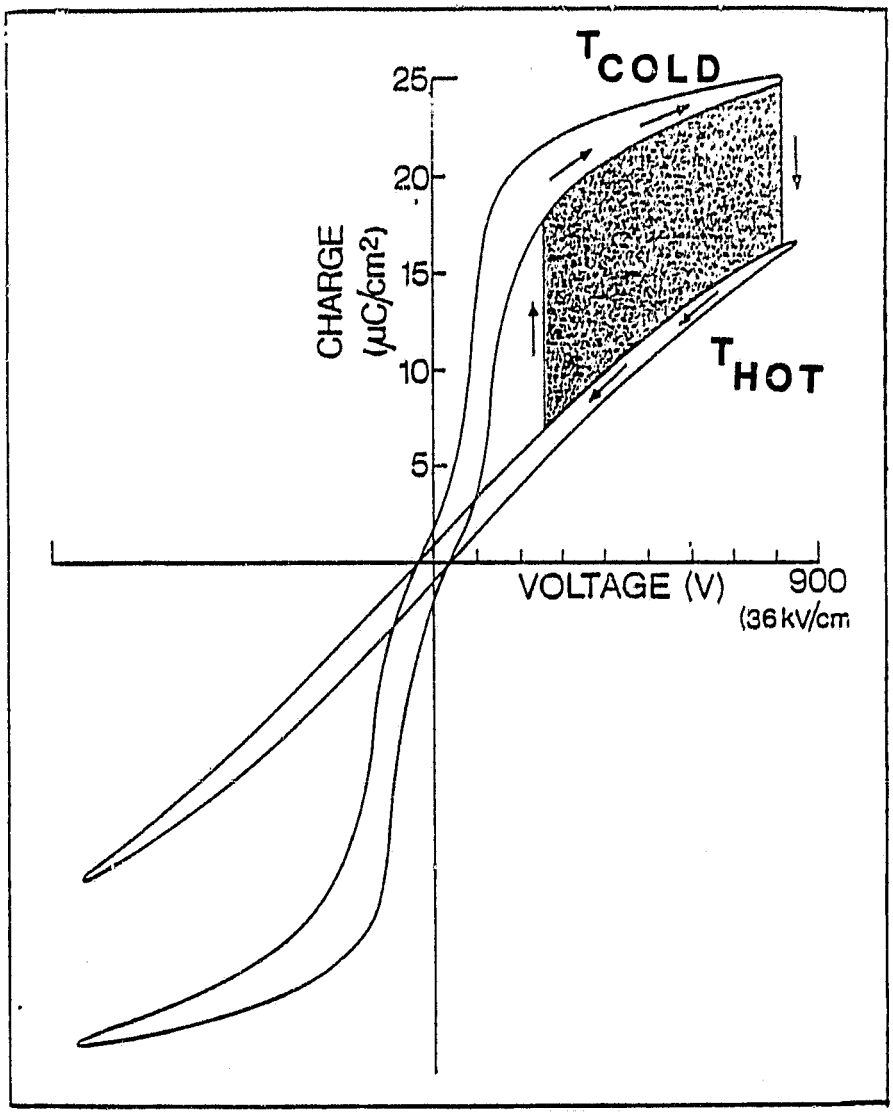

Fig. 2. An electrical energy production cycle may be realized by appropriately phased changes in temperature and applied electric field. The shaded area is equal to electrical energy per cycle which may be produced by $Pb_{0.99}Nb_{0.02}(Zr_{0.68},Sn_{0.25},Ti_{0.07})_{0.98}O_3$.

Now, however, an even more attractive pyroelectric material is appearing. Japanese workers (10), (11), (12), (13), (14) have reported the first polymer shown to have a clear-cut ferroelectric to paraelectric transition. Such a transition is necessary for highly active thermodynamic medium for use in pyroconversion. The name of the copolymer is vinylidene fluoride-trifluoroethylene and it is denoted as P(VDF-TrFE).

Thermodynamically, the copolymer is extremely impressive. The copolymer has a transition similar to that shown for the ceramic PZST in Figure 1 with a few important differences. One difference is that the transition (ferroelectric to paraelectric) occurs at 70 C rather than at 150 C. Much more importantly though, the dielectric strength of the copolymer is presently twenty five times greater than that of the ceramic. Since the electrical output energy density of the pyroelectric converter scales as the product of the electric field times the polarization, the higher dielectric strength of the copolymer represents a very important improvement. The present dielectric strength of commercial capacitor grade homopolymer P(VDF) is yet another five times greater (500 MV/m). As described later, it is expected that the copolymer dielectric strength will, with proper processing achieve comparable strength.

Before we discuss the space pyroelectric converter concept it is helpful to estimate the electrical output energy density which is possible using this new copolymer material. Since electrical output energy density is equal to the product of polarization density times electric field (corresponding to the area in Figure 2) the scale of this density is, (for the copolymer),

$$5\times10^{-6}\ \text{C/cm} \times 5\times10^{6}\ \text{V/cm} = 25\ \text{Joule/cm}^3$$

Actual cycles do not utilize the complete energy density calculated this way and are smaller by a factor of three or four. Thus we estimate that P(VDF-TrFE) may produce an impressive $7\ \text{J/cm}^3$ per cycle once its dielectric strength is improved to that of capacitor grade P(VDF).

SPACE STRUCTURES

Two types of structures were analyzed in this study. The first approach is illustrated in Figure 3. In its simplest version a pyroelectric converter can take the form of a rotating cylinder. A given segment of the cylinder will alternately rotate into and out of the direct sunlight. As a result, the temperature of the segment will rise (during the lighted time) and fall (due to reradiation) each revolution. If an externally applied voltage is raised and lowered in the appropriate phase relation to the temperature oscillation a substantial amount of electrical power

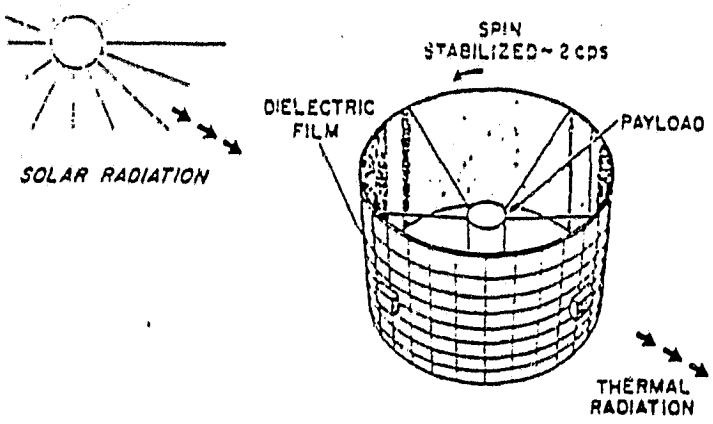

Figure 3 Illustration of a spacecraft application of radiant energy conversion using a thin pyroelectric film (8).

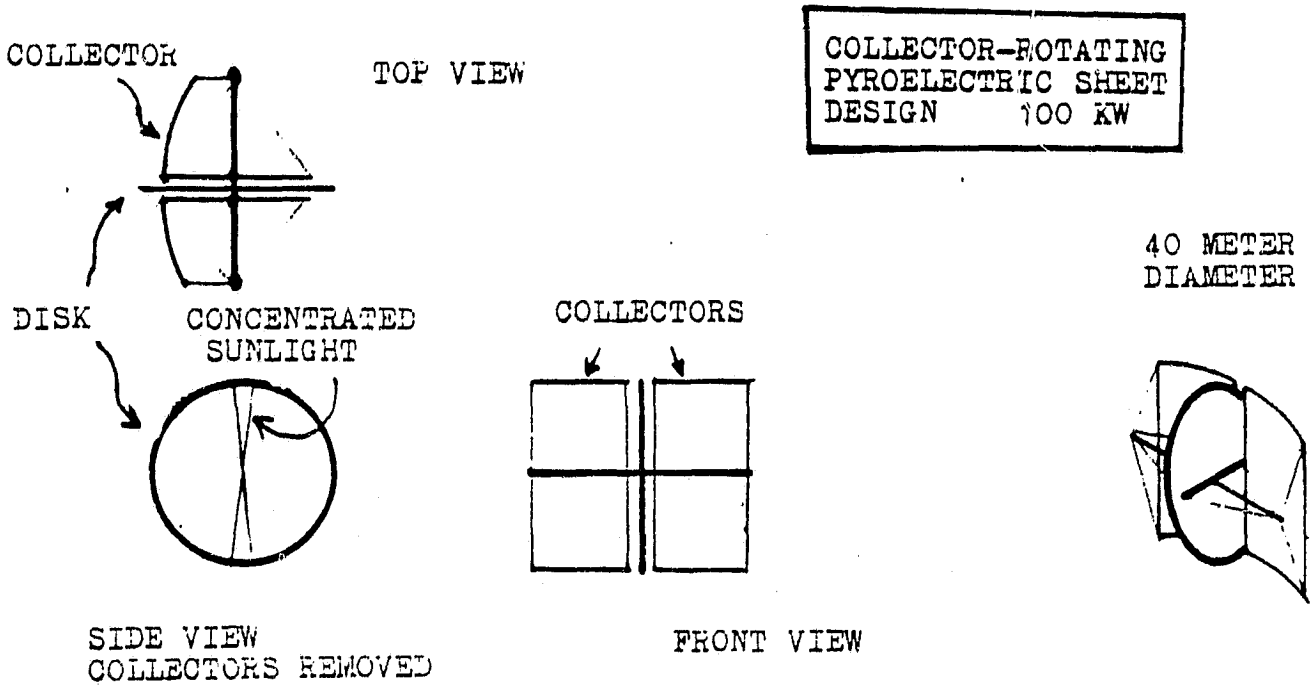

Figure 4 Collector and rotating pyroelectric sheet design (CS-2).

may be produced. Although this rotating cylinder design is attractive because of its simplicity, a somewhat more complex design may yield a greater power-to-mass.

The second structure is comprised of a rotating pyroelectrically active polymer sheet (in the shape of a disk) and a concentrating collector of sunlight. This collector plus sheet structure is called the CS-2 structure and is shown in Figure 4. (A precursor to this design involving a collector, rotating mirror and sheet was called the CS-1 structure.)

In the next section various "working" aspects of the space pyroelectric converter are examined. Later sections discuss power loss mechanisms, and system performance. The final section describes several special aspects of the pyroconverter which make it a particularly attractive electrical power generator.

Section 2

THERMAL, ELECTRICAL AND DYNAMICAL ASPECTS

HEAT FLOW

We have calculated the radiant transfer of heat into and out of the pyroelectric converter for the two configurations. Consider first the simple cylinder structure. The cylinder rotates at an angular frequency omega and a given spot on the outer surface receives heat input from the sun during the "daylight" half of the revolution. The input heat varies as a sinusoidal function of the angle between the incoming light and the surface (at the particular spot) on the cylinder. It was assumed that the inner surface of the cylinder was totally reflecting (i.e. emissivity equal to zero). Therefore, the various segments of the cylinder were radiatively decoupled. This assumption simplifies the calculation greatly. The resulting input of heat to a given segment during the "night" portion of the rotation is zero.

The heat output is governed by the Stefan-Boltzmann equation

$$\dot{Q}(\text{output}) = \epsilon \sigma T^4 \qquad (3)$$

where ϵ =emissivity, σ =5.67E-8 watt meter^{-2} kelvin^{-4}, and T=absolute temperature in degrees kelvin.

Figure 5 shows the results of a numerical calculation of the temperature extremes experienced by a segment of the cylinder surface as a function of the rotational frequency. The assumptions were; emissivity equal to 0.9 (independent of wavelength), volume specific heat of the cylinder surface equal to 3.0 megaJoule per cubic meter degree, pyroelectric sheet thickness equal to 10 micrometer, input solar power of 1300 watt per square meter. Also, an important simplifying assumption was used. The heat associated with the phase change (ferroelectric to paraelectric) was ignored. While this heat may be large (about 40 megaJoule per cubic meter for a Carnot limited conversion with a temperature swing of 50 degrees Kelvin at an input temperature of 400 Kelvin) it is about four times smaller than the sensible heat (150 megaJoule per cubic meter for a 50 degree Kelvin temperature excursion).

In order to achieve a temperature swing of 58 degrees the rotational frequency must be as slow as 0.13 Hertz. Notice that the temperature swing is approximately inversely proportional to the frequency over the illustrated parameter range. This result coupled with an output energy density (discussed in Section 3) which is linear in the temperature swing will yield an output power which is roughly independent of the rotational frequency over a restricted frequency range.

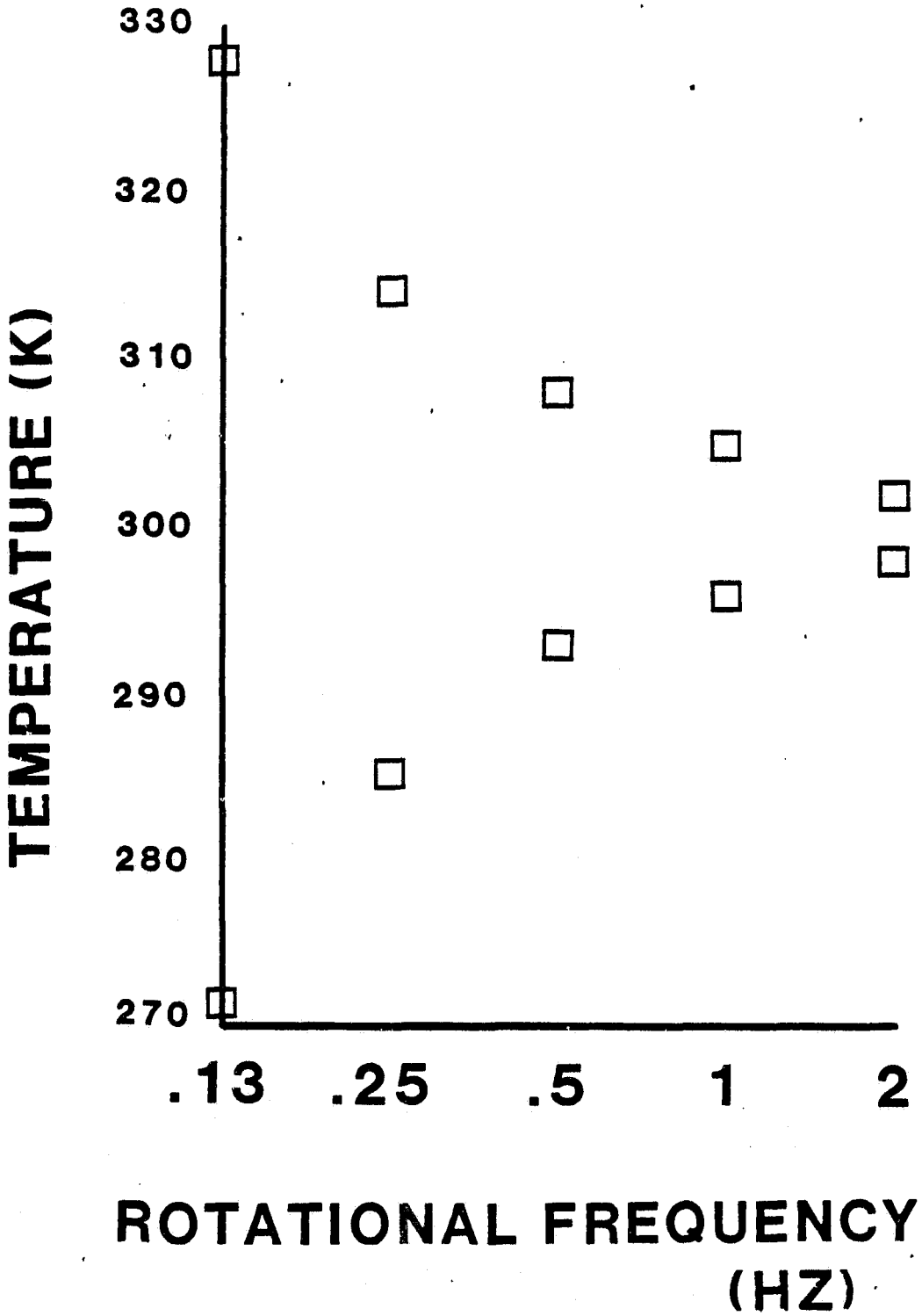

Figure 5 Temperature extremes of a segment of a rotating cylinder.

It is possible to estimate the maximum efficiency which may be obtained using this design (within the limiting assumption that the heat associated with the phase transition may be ignored). The calculated temperature swing for the 0.13 Hertz case was 58 degrees Kelvin. This temperature swing may be compared with the temperature swing which would occur if no reradiation were allowed during the heating process. Such a calculation yields a temperature swing of 110 degrees Kelvin. The ratio of the two temperature swings (58/110) sets an upper limit, within the simplifying assumptions, to the fraction of Carnot efficiency which may be achieved with the simple cylinder design. Thus one may estimate that the cylinder approach is limited to an energy conversion efficiency of about 50 per cent of the Carnot limit on the basis of heat transfer alone. This is not necessarily an extreme disadvantage for this design since efficiency alone is the not the prime parameter for a space power system. What this does mean though, is that the cylinder design suffers a penalty of almost a factor of two in power-to-weight compared with concentrator pyroelectric designs.

The second configuration for which we studied the heat flow was the CS-2 (concentrator and rotating pyroelectric sheet). In this case a concentrator focuses heat onto a restricted area of a rotating pyroelectric disk. The portion of the disk which is within the wedged shaped concentration zone heats up rapidly. As soon as that portion of the pyroelectric disk leaves the concentrator zone it begins to cool slowly by reradiating. Due to the concentrator geometry and the temperature of the heat source (i.e. the sun at about 5000k) the heat up zone takes up only a small angular wedge of the pyroelectric disk. The computer code that we have written has among its variables the collector concentration ratio, and the angular size of the heat up zone.

For example, for the conditions;

concentration ratio = 8
frequency = 1 Hz
wedge fraction = 0.1 (heatup angle = .63 radian)
sheet thickness = 10 micrometer

the resulting temperatures for the pyroelectric sheet disk are,

low temperature = 300K = 27C
high temperature = 330K = 57C
temperature swing = 30K.

An estimate of the radiative heat transfer limit on the conversion efficiency as was shown earlier for the cylinder case yields (30/35) 86 per cent of the Carnot limit. Thus, only about 14% of the heat leaks away during the heating portion of the cycle as compared with nearly 50% calculated for the simple cylinder design.

It is important to note that an advantage that the CS-2 design has over the simple cylinder is that the CS-2 approach has an extra design parameter, the input power per unit area (the concentration ratio combined with the concentration zone angular size). This extra parameter allows the designer to set the average temperature of the converter. If we refer back to figure 1 for the cylinder design notice that the average temperature is essentially fixed (for a spacecraft at a given distance from the sun). This flexibility of the CS-2 design allows the spacecraft temperature to be set to optimize the output performance of a given pyroelectric material (the pyroelectric material should operate in a temperature range which spans the ferroelectric to paraelectric transition).

Figure 6 shows the average temperature of the pyroelectric sheet (in the CS-2 design) as a function of the concentration ratio of the collection optics. The assumptions of the plot are that the thickness of the sheet is 10 micrometer, the frequency of the thermal cycle is one Hertz, and the wedge of concentrated incoming light impinges upon one tenth of the area of the sheet . The average temperature is very insensitive to the frequency of the thermal cycle. The amplitude of the temperature swing which is also shown in Figure 6 does, however, depend upon the frequency of the thermal cycle. The amplitude of the temperature oscillations is approximately proportional to the period of the thermal cycle.

It is useful to note that the abscissa of the figure 6 corresponds to the input thermal power of the pyroelectric converter. Thus the average temperature of the pyroelectric sheet is determined once this input heating power is set. Conversely, the input thermal power must be controlled so as to result in the proper operating temperature for a given pyroelectric material. As with all space power systems, higher temperatures correspond to higher thermal power per unit area of radiator.

One important difference between the simple cylinder and the CS-2 design is that the radiated power per unit area for the CS-2 design is double that for the cylinder approach for any given temperature. The reason for this is that the CS-2 pyroelectric sheet can reradiate from both its front and back sides. The cylinder, however, has only one surface which views deep space.

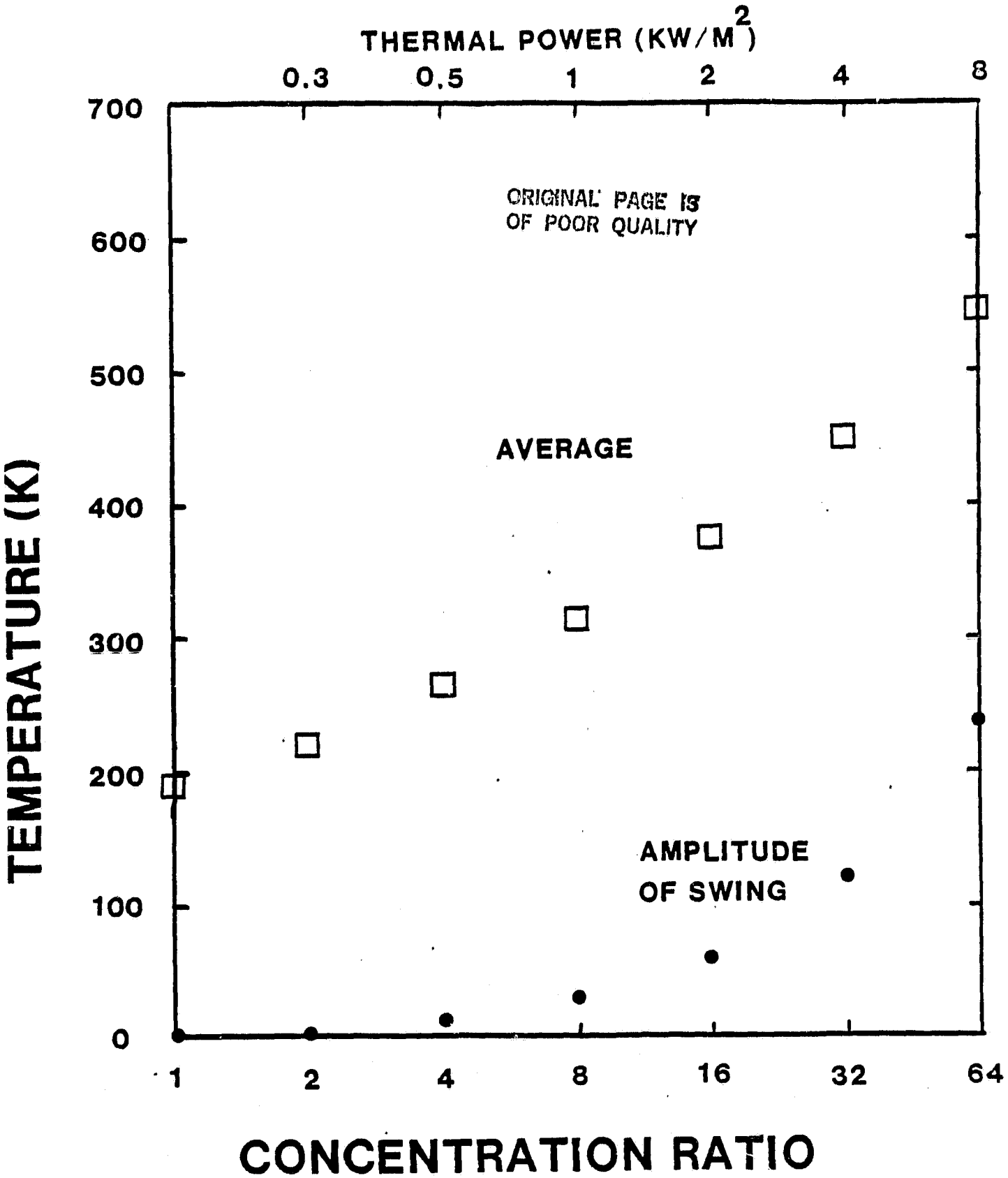

Figure 6 Average temperature of the CS-2 sheet as a function of concentration ratio of the collecting optics.

POWER EXTRACTION

The key element of the power extractor is essentially a switching power supply. The high efficiency of such power supplies (developed by NASA) is well known (see for example (15). For our purposes, switched-mode power conversion may be thought of as simply an efficient way to transform energy at one voltage into energy at another voltage. As this efficient energy transformation occurs, a transfer of charge takes place. The charge moves from one place and voltage in the circuit to a new place and voltage in the circuit. As the charge is transferred the number of Coulombs changes so as to (approximately) conserve energy.

A simple version of a switched-mode power convertor is illustrated in figure 7. To the left is a capacitor (C1) initially charged to some high voltage. To the right is another capacitor (C2) initially uncharged. If the switch is momentarily closed, then current begins to flow through the inductor. After only a very short time (a time less than the resonant time for the capacitor - inductor pair) the switch is reopened. What has happened? Energy has been passed from the capacitor to the inductor. In the next moment energy passes from the inductor to the capacitor (C2) as the current now flows though the diode. The net result is that energy in the form of charge on capacitor (C1) has been transferred to energy stored on capacitor (C2). It turns out that the transfer may be done very efficiently. Note that simply connecting the two capacitors directly together (without an intermediate inductor) would have resulted in a loss of 50% of the transferred energy. With this brief introduction to switched-mode power conversion in hand we next discuss the approach for power extraction from the pyroelectric generator.

The reference points for an extraction cycle are given on a charge-voltage diagram in figure 8. The temperature excursions during a cycle are shown in figure 9. The temperature history in figure 9 corresponds to that of a point within the sheet of a concentrator type design. The rapid increase in the temperature between points 0 and 1 is indicative of the concentrated heat input. Similarly, the much slower temperature decline between points 2 and 3 indicates the slower process of reradiation of heat out to deep space.

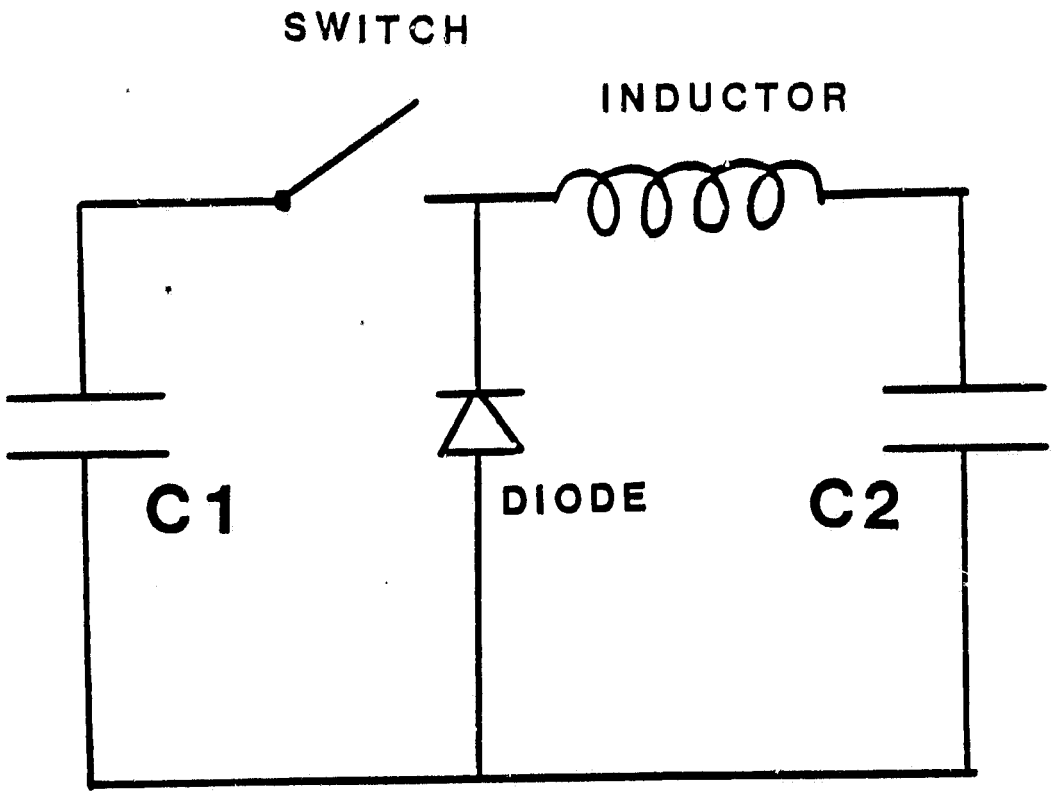

Figure 7 Simple version of a switched-mode power converter.

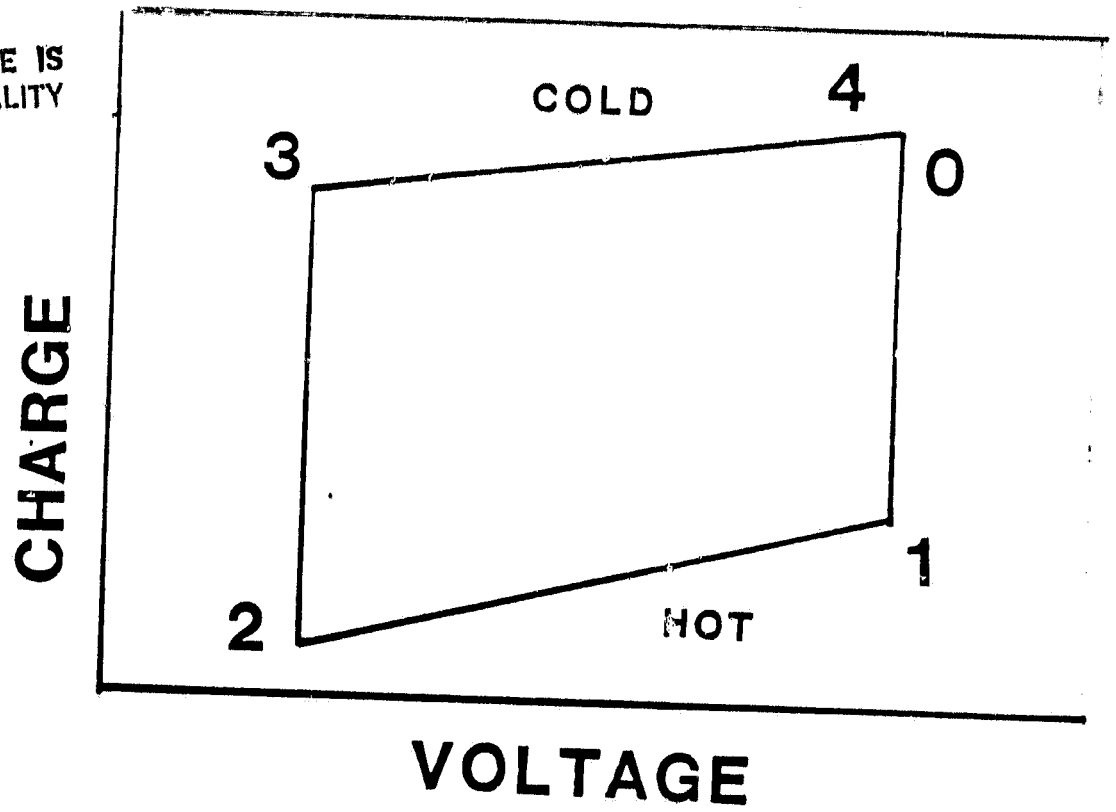

Figure 8 Reference points for an extraction cycle are given on a charge-voltage diagram.

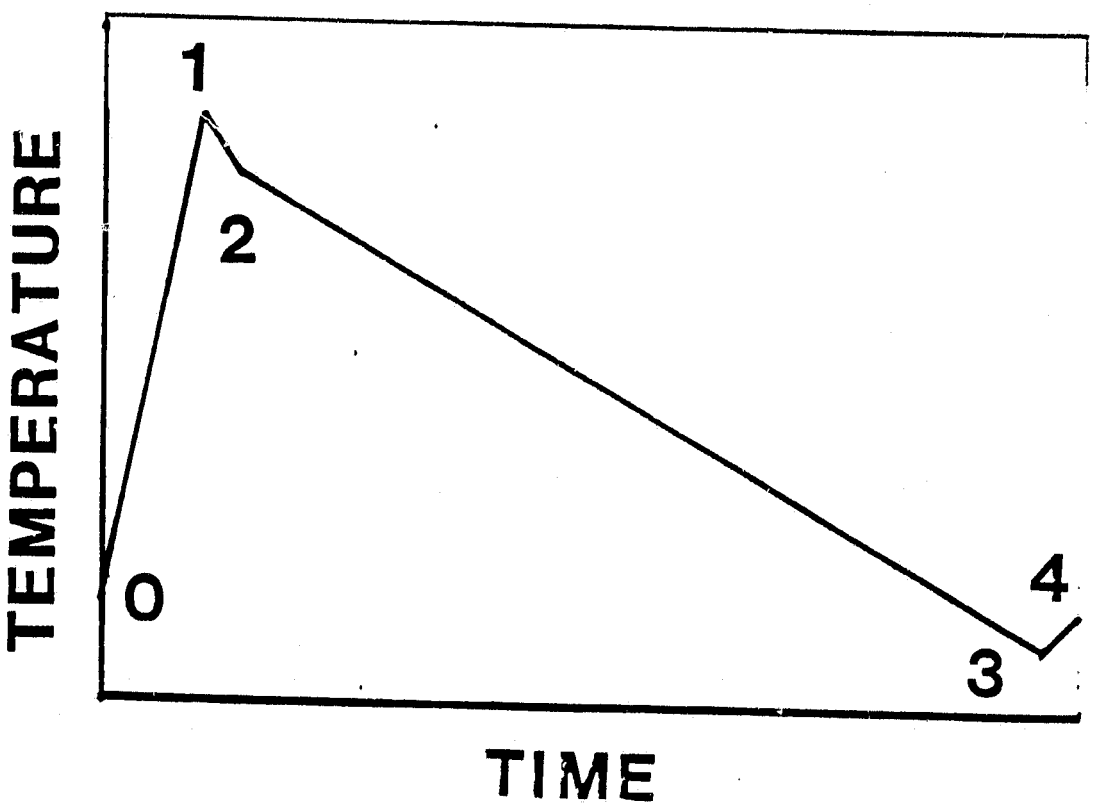

Figure 9 Temperature excursions during a cycle (for the CS-2 design).

For optimum efficiency in the transfer of power from a pyroelectric generator to a useable power output bus, there will be several separate pyroelectric generator segments.

The voltage profile and power extraction profile for an individual segment are shown in figures 10 and 11 respectively. The voltage during power extraction will remain approximately constant for the period of time between points 0 and 1 as shown in figure 10. For a 10 micrometer thick pyroelectric sheet which is stressed to 300 MV/m the extraction voltage would be 3000 V. As power extraction continues, the voltage will drop to some lower point marked by point.2. At the same time as this lowest voltage is reached, power becomes available from the next segment for collection. Also, at this point further power extraction from the first section stops and a recharge cycle begins. The geometry and number of these sections will be arranged so that one segment is always at a high voltage potential and in an extraction mode at the time that another section or sections must be brought up to high voltage by adding charge. This time is indicated by points 3 and 4 in figure 10.

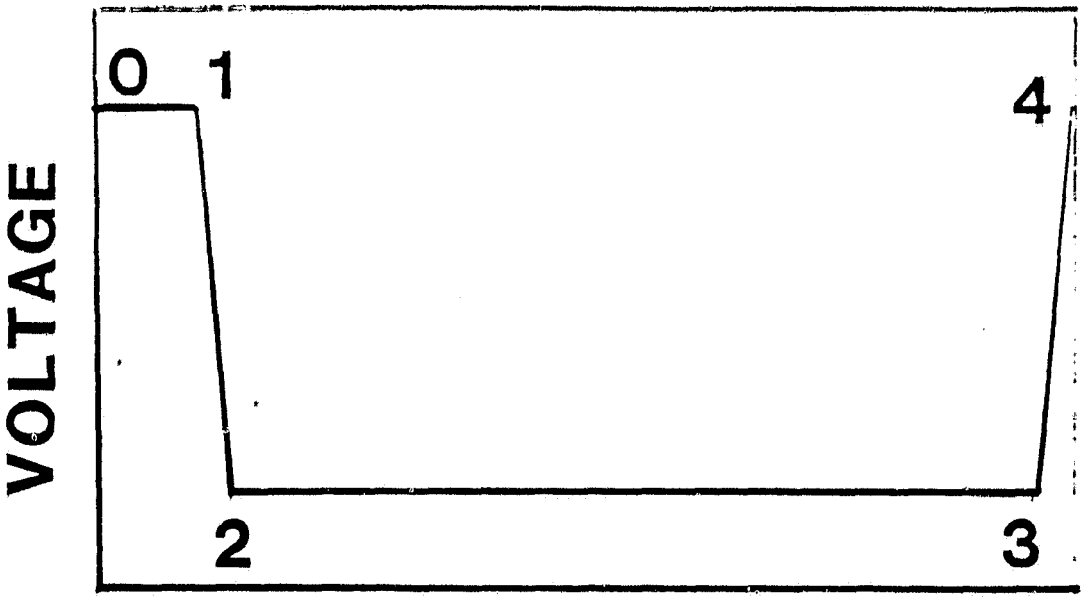

Figure 10 Voltage profile for an individual segment of the pyroelectric disk.

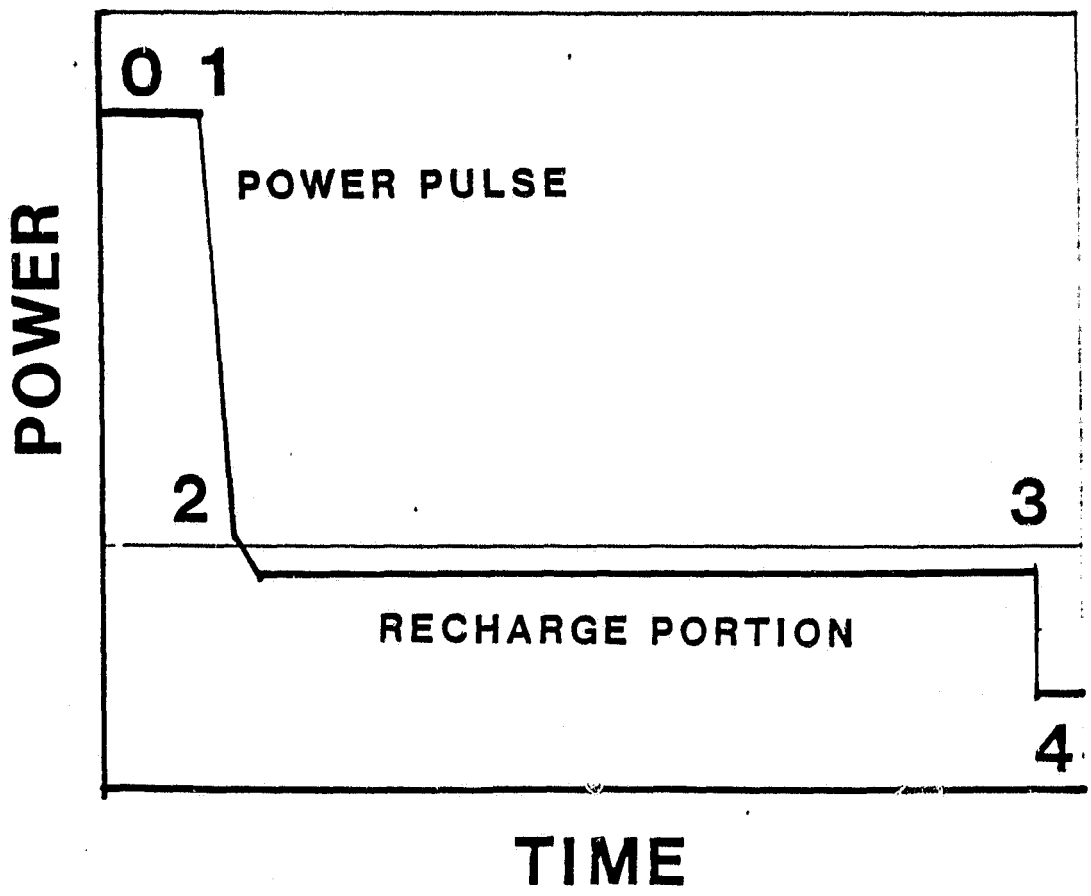

Figure 11 Power extraction profile for an individual segment of the pyroelectric disk.

A simplified circuit design which can accomplish both power extraction and pyroelectric generator recharging is shown in figure 12. A central bus (point A) is fed from the several individual generators (only four are shown). Whenever a particular generator is at high voltage and ready to begin extraction, the SCR switch is closed thereby transferring this section's voltage onto the central bus. Because this transferred voltage is higher than that of the previous segment (which has become almost depleted), the previous contributor to the bus is back biased thereby going off (i.e. opening that switch) until it is again gated on by the controlling circuit. This new section then contributes output energy until it is also depleted and replaced by the next in a repetitive cyclical manner. During the balance of the cycle time, i.e. when a segment is not contributing power, the segment is recharged. Figure 10 illustrates the power required for this recharge cycle (from point 2 to 4). This recharge is accomplished by high voltage, high frequency switching regulator as depicted by FET 1 (field effect transistor) and inductor L1 (the recharging diodes are not shown). This regulator is "programmed" to recharge each segment utilizing power from the central bus. Energy efficiency during recharging should be high, perhaps 95%. It is also important to realize that the recharging energy will be only some fraction of the output energy. Therefore the 5% recharging energy loss applies only to a fraction of the output energy. The switching regulator will be programmed in order to profile both the recharging voltage and coulombic transfer as depicted by figure 10 and 11.

Finally, the extractor power on the central bus must be conditioned in order to remove the high percentage of low frequency ripple. This can be accomplished by using high frequency switch regulators made up of components FET 2, L2 and C3. The output from this power conditioning and regulating circuit will be slightly lower than the lowest voltage on the central bus. Extraction could typically reduce the voltage on a given segment down to approximately 500 volts resulting in a final user bus voltage of about 400 volts. This output conditioning could be done at 95% efficiency.

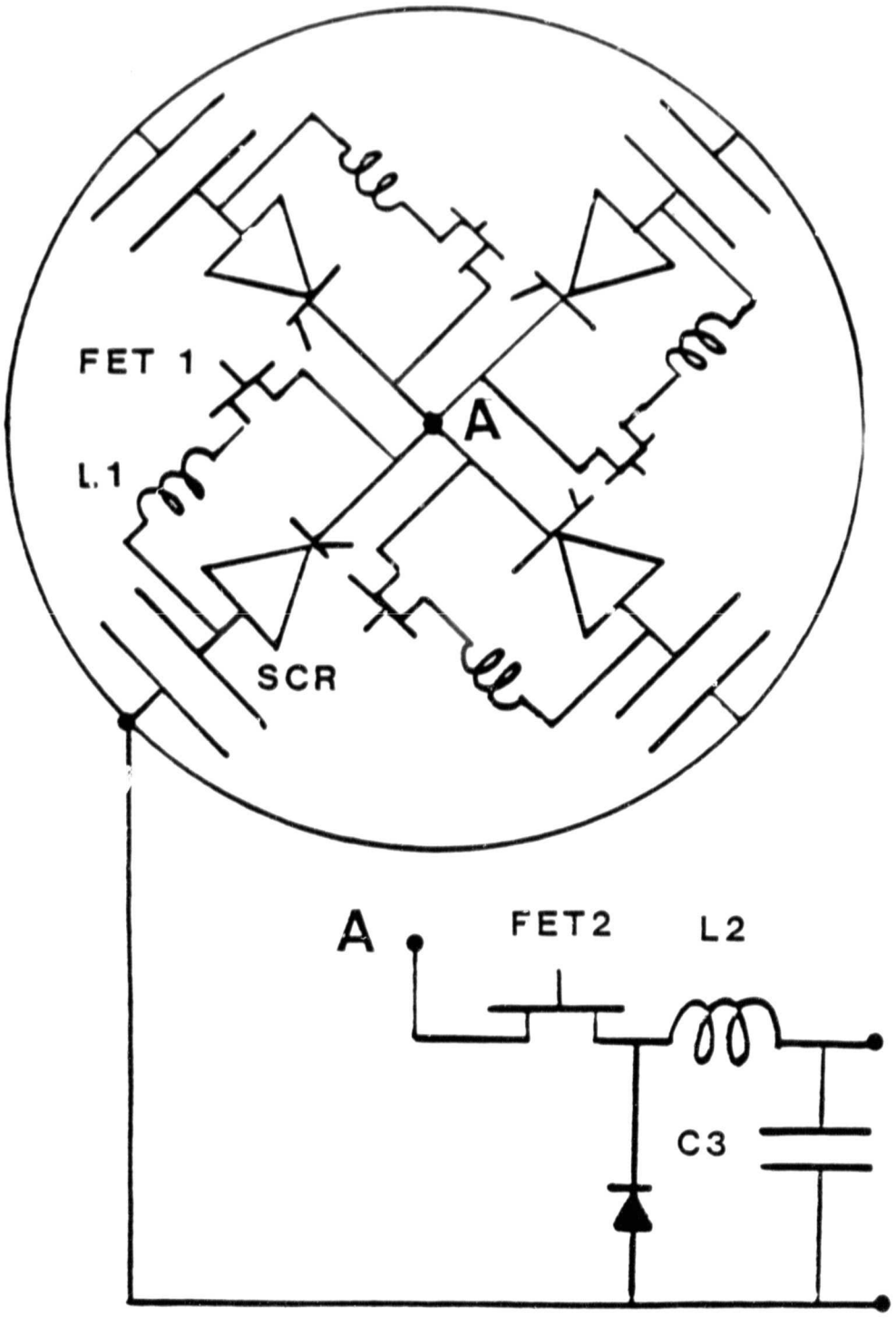

Figure 12 Simplified circuit design which can accomplish both power extraction and pyroelectric generator recharging.

ELECTRODE RESISTANCE

The pyroelectric converter is a high voltage device. This high voltage nature is an advantage in terms of current collection. Simple calculations have been made to determine the sheet resistance of thin electrodes on the surfaces of the pyroelectric sheet. The results indicate that sheet resistance effects (Joule losses) will be negligible. For the conservative CS-2 design the losses in the electrical lead wires were more important than the sheet losses. The lead losses may be set to any desired level simply by sizing. Wire sizes of the order of 10 to 12 gauge (about a millimeter in diameter) for aluminum and copper, respectively, correspond to power losses which are one percent of the output power. These wire sizes are for the individual segments on the pyroelectric sheet. For a 100 kilowatt CS-2 design (conservative 2% efficient version), this yields the mass of the conducting wires at 8 to 16 kilogram. Thus sheet resistance is unimportant (no need to lay down elaborate current collecting grids) and the current leads may be very lightweight without causing undue power losses.

POINTING DYNAMICS AND DRAG

The rigid body dynamics of a spacecraft in the near earth environment is, of course, a well studied subject. An excellent paper on this subject is presented by Wildman (16). Not only has Wildman studied the drag and torque on a spacecraft but he has also considered the effects of rotation. It turns out that the spin reducing drag is a very small effect at least for rotational speeds similar to those which were used in the Echo spacecraft. The dominant torque effect which we must contend with is the gravity gradient torque. This torque may, in principle, be eliminated by arranging for all of the moments of inertia of the spacecraft to be equal.

Apart from torque effects upon the spacecraft the most important rigid body dynamic aspect is that of altitude reduction from straightforward drag. Photovoltaic arrays orbiting at altitudes of the order of 500 km will have decay rates of between 0.2 and 2 km/day. Since the pyroelectric systems will be lighter per unit area they're decay rates will be even faster. Fortunately, the orbital decay rates drop by a factor of 100 if the altitude is increased by only 200km. Therefore, though the very lowest altitudes do not appear to be reasonable locations for the use of the pyroelectrically powered spacecraft, this restriction upon the altitude is rather minor.

Section 3

LOSS MECHANISMS

PLASMA INTERACTIONS

Plasma conduction loss

The two aspects of electrical interaction between the high voltage of the pyroelectric spacecraft and the space plasma are the power loss and the threshold for the occurrence of arcing. The existing information in this area has been obtained with an eye toward photovoltaic applications. However, several of the results of the photovoltaic studies can be applied with caution to the pyroelectric converter.

We begin by considering the power loss due to the finite conduction of the near earth plasma. Even though the "vacuum" above 500 km is ultra high by laboratory standards, its current carrying capacity may be substantial. An oversimplified model of the conduction current might read as;

$$J = Ne(2eV/m)^{1/2} = NeS \qquad (4)$$

where J is the current density, N is the density of electrons, e is the charge of an electron, V is the voltage of the spacecraft surface relative to the plasma, m is the mass of the particle (either electron or ion) and S indicates the speed of the particles as they impact the spacecraft. For low earth orbit (LEO) conditions, this equation yields 10 amp per square meter for a voltage of +10,000V. The corresponding power loss is, of course, tremendous at 100 kilowatt per square meter. Even for the heavier oxygen ion current this simple equation yields a huge power loss of 560 watt for a negative voltage of -10,000V.

McCoy (17) gives a good account of the many factors which limit the current, and hence the power loss, to a much smaller value than the previous simple model of equation (4). Among these factors are collisions, magnetic field effects, orbit-limited current collection (arising from particle angular momentum about the collecting probe), and space-charge effects. The space-charge effect is particularly important for large area spacecraft. When a large area is maintained at a high potential relative to a plasma, the charged entities rearrange themselves so as to screen out the high electric field. The screen region is normally referred to as the sheath. The entire difference in potential between the high voltage surface and the surrounding plasma becomes concentrated within this sheath. The total ion current collected is limited to the ions that cross the outer boundary of the sheath as a result of their existing thermal or drift motions in the undisturbed plasma. The thickness and therefore the area

of the outer surface of the sheath can be calculated from space-charge equations.

It turns out that the sheath thickness depends upon the voltage of the surface; the higher the voltage, the thicker the sheath and the larger the effective collecting area. For small objects the growth in the sheath size with voltage can be quite substantial. Fortunately, for large area surfaces, the same growth in the thickness of the sheath results in only a small increase in the effective collecting area.

The result of all of this is that the large power losses which one might expect by erroneous scaling of small probe plasma experiments do not occur.

McCoy (17) studied the sheath in a large area laboratory experiment (Fig. 13). Figure 14 shows some of his measurements of current collection for a 10 square meter solar power satellite (SPS) surface in fairly high density plasmas. From the figure one can estimate the power loss to be between 0.1 and 10 watts per square meter depending upon the plasma density. The plasma density limits correspond the range of altitudes from LEO to the near Van Allen belt as shown in figure 15. Stevens (18) also studied simulated solar cells at high voltage in plasmas of approximately the same conditions and found power losses of about 0.1 watt per square meter for a negative -1000V potential and a loss of about 10 watts per square meter for a positive +1000V potential. Stevens (18) found a good correlation between his lab data and the PIX spacecraft test data as shown in figure 16. Freeman (19) estimated that the power losses for a photovoltaic SPS configuration operating at tens of kilovolts will be 9 watts per square meter in LEO and about 0.1 watt per square meter in geostationary earth orbit (GEO).

In summary, the losses are expected to be in the range of 0.1 to 10 watts per square meter. The upper limit of that range would present a problem for the pyroelectric converter since it would represent a loss of between 8% and 33% of the produced power for the CS-2 design (and could potentially extinguish the cylinder design output).

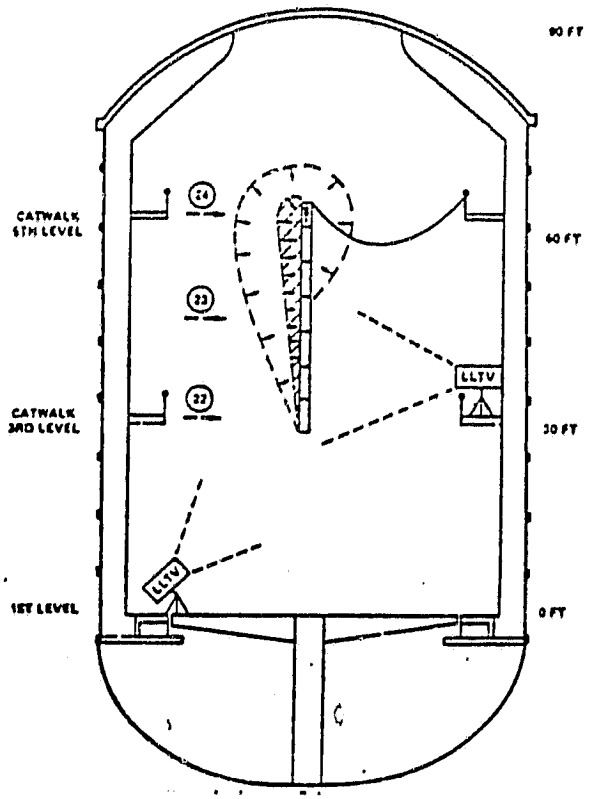

Figure 13 High voltage array test set-up in chamber (17).

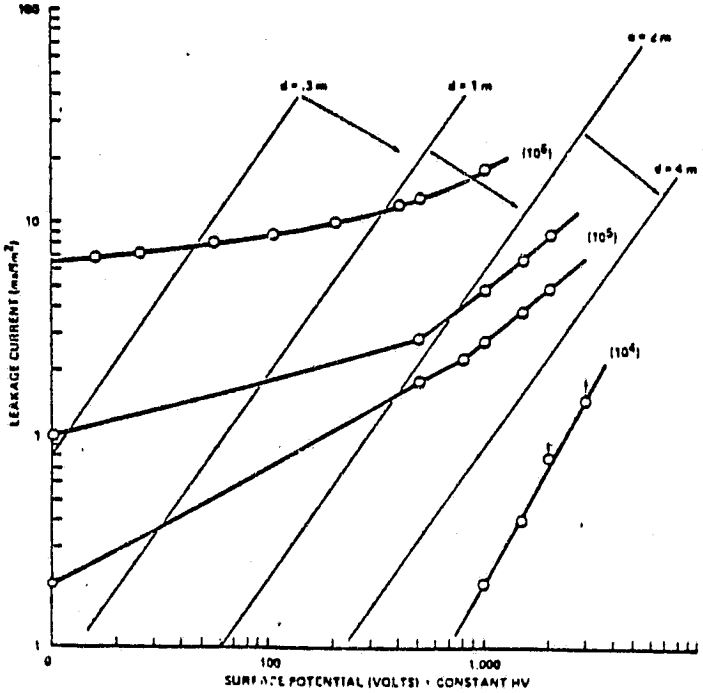

Figure 14 Measured current leakage from "SPS" to plasma (17).

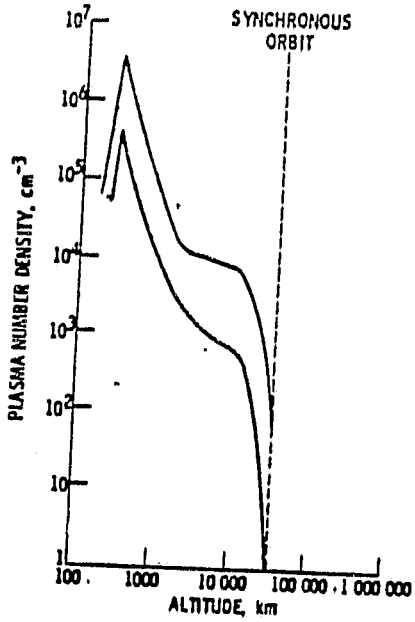

Figure 15 Plasma number density vs. altitude in equatorial orbit (18).

INTERACTIONS OF SPACE STRUCTURES WITH ENVIRONMENT

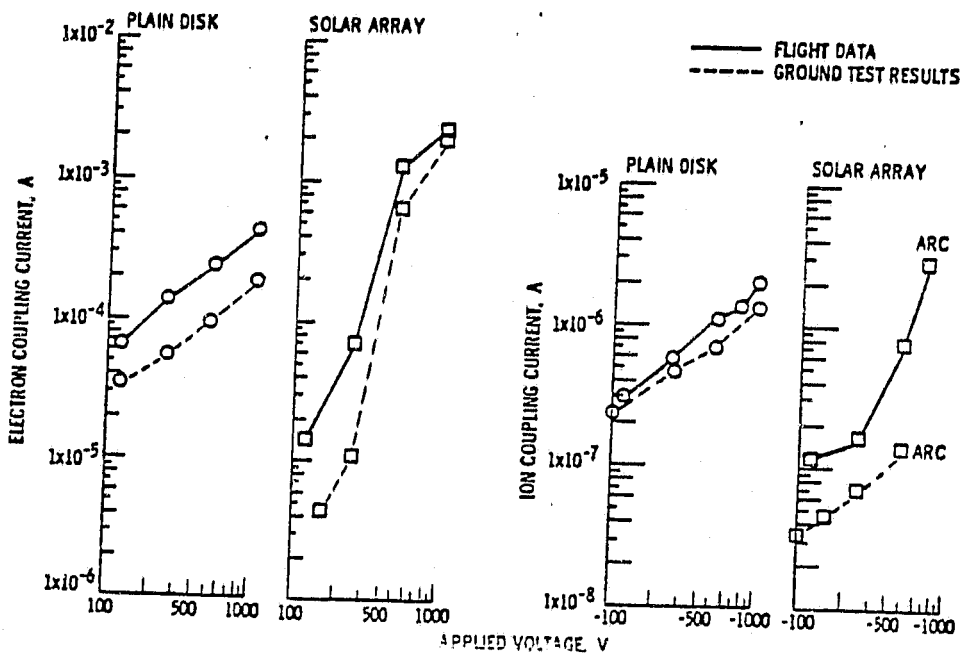

Figure 16 PIX flight results (18).

Plasma arcing

Arcing was observed in McCoy's (17) laboratory experiments for voltages exceeding either +400V or -5000V. All of those arcs, however, were observed to originate at insulating surfaces. Note also that McCoy's experiments were performed under LEO type plasma conditions.

In Stevens' (18) measurements (also LEO conditions) arcing was observed at -500 to -1000V (in this case from conductors) while no arcing was reported for positive potentials up to +1000V. This group estimated that the threshold for arcing at GEO will be at -5000 to -10000V.

Reiff (20) also does "not anticipate anomalous arcing in the GEO environment". And Purvis (21) made no mention of arcing for the ATS-5 and 6 spacecraft even though they measured charging potentials of up to 20 kilovolts for these vehicles in GEO.

Unresolved questions

If high voltage interactions with the plasma are important then why can we not consider embedding the high voltage within the bulk of the pyroelectric material? This two sheet approach, with an inner high voltage electrode and a pair of "grounded" outer electrodes, is worth a bit of consideration. Pinholes in the sheet, for the dual sheet design, may give rise to plasma losses which are comparable to an exposed sheet due to current focusing which apparently occurs within the space-charge sheath.

How large must the unelectroded edge region of the pyroelectric sheet be? Large insulating surfaces on spacecraft appear to be invitations to arcing. On the other hand, small "capacitor" edges will necessarily invite surface conduction losses.

PYROELECTRIC LOSS MECHANISMS

Ferroelectric Hysteresis

In the course of a pyroelectric conversion cycle, the electric polarization is constantly changing (in response to thermal and electric field changes). Though the polarization changes are expected to be nearly reversible, in a thermodynamic sense, the reversibility will certainly not be perfect. To the extent that the polarization is not perfectly reversible, some electrical energy (which might otherwise be generated) will be lost. This irreversibility gives rise to the ferroelectric hysteresis loss.

It is important to emphasize that the ferroelectric hysteresis loss which accompanies a pyroelectric conversion cycle is **not** the same as the energy associated with the standard ferroelectric hysteresis loop.

The extent to which ferroelectric hysteresis effects the power production cycle in the copolymer is currently not known. The only detailed measurements that have been made on the hysteresis which is relevant to pyroelectric conversion are the measurements of Olsen and Evans (22) on ceramic lead zirconate modified with tin and titanium (PZST). The measurements on PZST indicate that the hysteretic loss is small, about 8% to 16% of the output electrical power for that ceramic. This result is only suggestive of what the case might be for the copolymer.

One experiment which has been performed on the copolymer gives a small hint as to the possible extent of hysteresis loss during the pyroelectric cycle. While in the course of a standard ferroelectric hysteresis study (wherein the electric displacement is measured versus a cyclically applied electric field) we have measured the displacement for small, unipolar, excursions of the electric field. The ferroelectric hysteresis associated with these unipolar excursions is very small even for the case where the minimum electric field approaches zero. Such isothermal unipolar excursions, of course, do not address the question about the reversibility of the polarization under varying thermal conditions. It is possible that the low voltage limit for the repoling (polarization increase during cooling) process of the pyroelectric conversion cycle may be very nearly equal the to high voltage limit. Though we currently do not expect this to be the case, only an experiment can tell for certain. Rather than a catastrophic reduction of the predicted output energy density we expect that the impact of the ferroelectric hysteresis loss upon the converter to be minimal, perhaps amounting to 10% of the output power.

Bulk Conduction Losses

The power loss due to electrical conduction through the bulk of the pyroelectric material is the Joule loss represented by

$$\text{Joule loss} = E^2 / \rho \qquad (5)$$

where the Joule loss power (V^2/R in unnormalized terms) is stated per unit volume of pyroelectric material, E is the electric field, and ρ is the bulk resistivity. The equation looks very simple but the resistivity is a function of both temperature and electric field (the materials are not generally simple ohmics at the high electric fields expected for the pyroelectric converter). Calculation of the Joule loss is further complicated by the fact that the temperature and field are continually changing during the course of the conversion cycle.

To get some feel for the power loss numbers consider figure 17. Plotted in figure 17 are constant power loss contour lines for various values of resistivity and electric field. The power loss values are denoted next to each line. Note that the power loss is greater for larger fields and smaller resistivities. Also

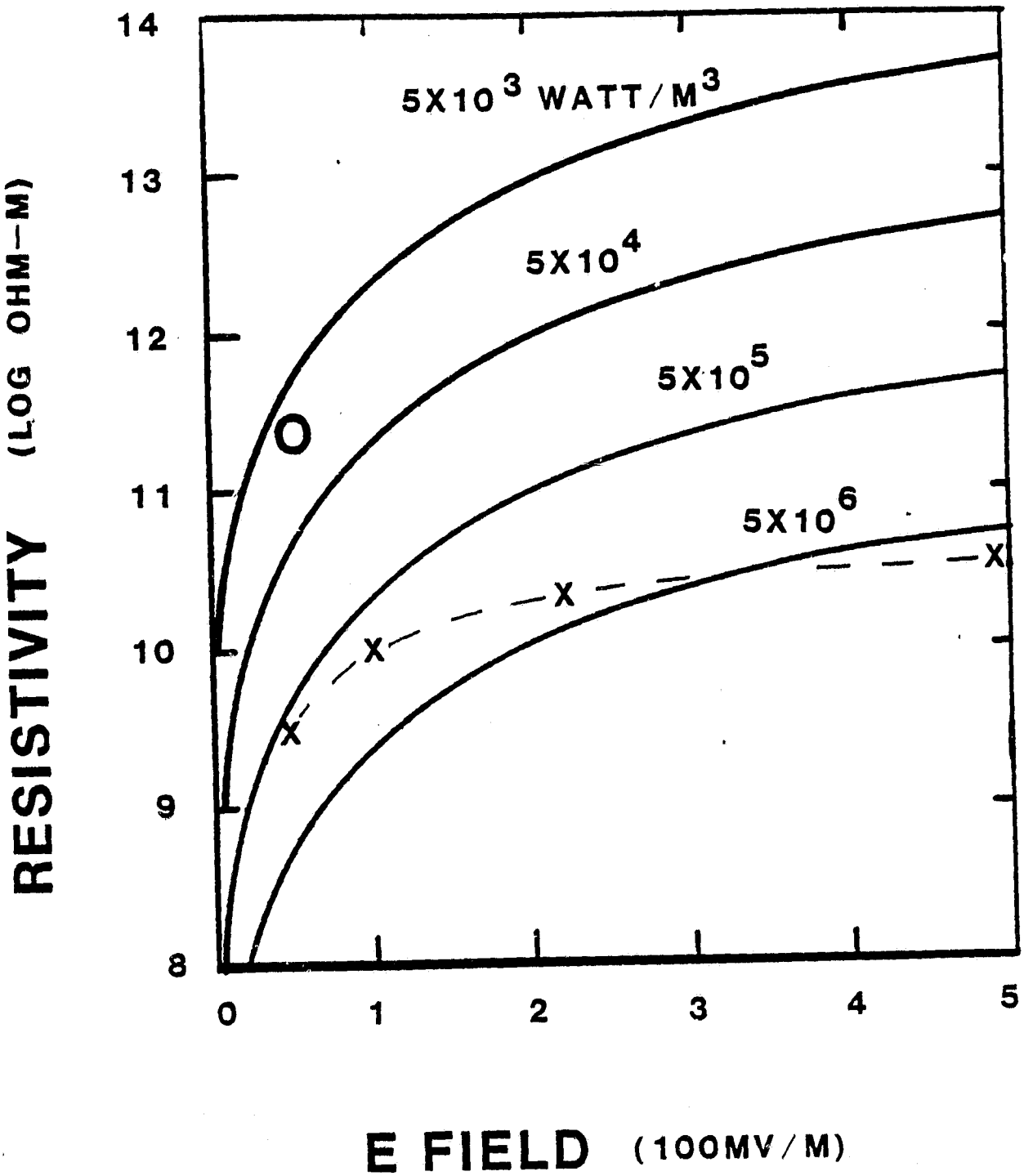

Figure 17 Constant power loss contour lines for various values of resistivity and electric field.

note that the solid contour lines are shown for each factor of ten in the power loss. For comparison the projected output power density points (shown as x in the figure) are included. The dotted line connecting the output power points is, of course, not a constant power line but rather a linear function of the electric field (according to the approximation of Section 4) using a temperature swing of 50K and an assumed frequency of one Hertz.

Figure 17 is useful for picking target resistivities for various operating fields. For example, let's say that we desire the Joule losses to be less than one per cent of the output power density. Once the power density is located on the figure, then the desired resistivity is that which lies two contour lines above.

The circle at a resistivity of 3×10^{11} ohm-meter and 5×10^{7} V/M corresponds to the present value of resistivity and electric field strength. It is seen from figure 17 that if it is possible to achieve about the same resistivity at a 500 megavolt per meter electric field then the Joule loss may be of the order of ten per cent. Actually, when the thermal cycle timing details are taken into account, it is realized that for CS-2 approach (in which the pyroelectric material spends only about one tenth of the time at high fields) the Joule loss may be more on the order of one percent.

Conduction Loss Mechanisms

Recent studies on electrical conduction in PVDF by Oka and Koizumi (23), Saito et al. (24) and by Olsen et al. (25) are consistent with the concept of ionic conduction. The origin of the impurity ions in polymers is considered to be mainly polymerization catalysts and decomposition products of the polymer. Trace amounts of other ionic contaminants may be picked up during the various synthesis steps. It has been suggested (26) that Na, Al and Si are major contributors to the ionic conductivity in a polyimide. Also, Kosaki et al. (27) concluded that fluorine ions are the main charge carriers in PVDF. Osaki et al. (28) pointed out that Na, Ca, Al, S, and Cl are present in PVDF as trace impurities.

The following excerpt from Blythe (29) elucidates several important aspects of ionic conduction in polymers.

"The most definitive evidence for ionic conduction is the detection of electrolysis products formed on discharge of the ions as they arrive at the electrodes. Unfortunately, the very low level of conductivity in polymers generally precludes such detection. Even at a conductivity of 10^{-9} mho m^{-1}, and we must bear in mind that many polymers exhibit conductivities several orders of magnitude lower than this, 100 V applied across a

specimen $100\ mm^2$ in area and 1 mm thick would only produce about $10^{-11}\ m^3$ of gas at NTP per hour. We therefore have to rely on rather more indirect means of elucidating the mechanism of conduction.

When the conductivity in question is very low, there are other experimental difficulties too. On application of a step voltage across a specimen, the initial current may be dominated by a displacement curreht due to polarization of the material. Since some dipole orientation may be very slow to reach equilibrium, the displacement current can swamp a small conduction current for a long time. Taking into account the drift characteristics of a practical measurement system, we can appreciate that in extreme cases a steady current reading will never be obtained, and a direct measurement of conductivity will not be possible.

Some physical insight into what a conductivity of around 10^{-9} mho m^{-1} or less entails may be gauged through the equation.

$$\text{conductivity} = q\ n\ \mu \qquad (6)$$

where q=charge, n= concentration and μ = drift mobility of the carriers. We can tentatively use a mobility value of the order of $10^{-9}\ m^2\ V^{-1}\ s^{-1}$, as found for ionic carriers in hydrocarbon liquids at room temperature. Although we would expect the true value for solid polymers to be lower, it should not differ by more than a factor of 100 or so for small ions. Then, assuming that the ions carry a single electronic charge, substitution in equation (6) gives a carrier concentration of $10^{19}\ m^{-3}$. Comparing this with the typical number density of molecular repeat units (nominal molecular weight=100) of about $10^{28}\ m^{-3}$, we can see that an exceedingly low carrier concentration is implied. This means that degrees of ionic impurities which may be totally ignored in the context of other properties may have a significant effect on conductivity."

Thus impurity levels as small as one part per billion may be important.

With the foregoing cautions regarding experimental difficulties in mind, consider a particular method for obtaining evidence for ionic conduction. A simple model of Mott and Gurney (30) describes the dependence of current on applied voltage as

$$J = A \sinh(eaE/2Kt) \qquad (7)$$

where J is the current density, $eaE/2$ is the change in barrier heights described in figure 18, "a" is the distance between neighboring potential wells, e is the charge of an electron, E

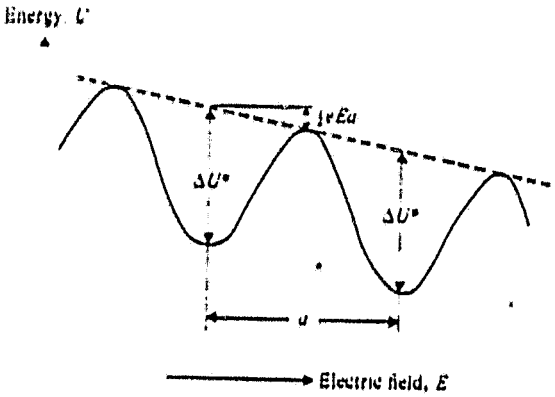

Figure 18 Diagram showing the deformation of ionic potential-energy well by an applied electric field.

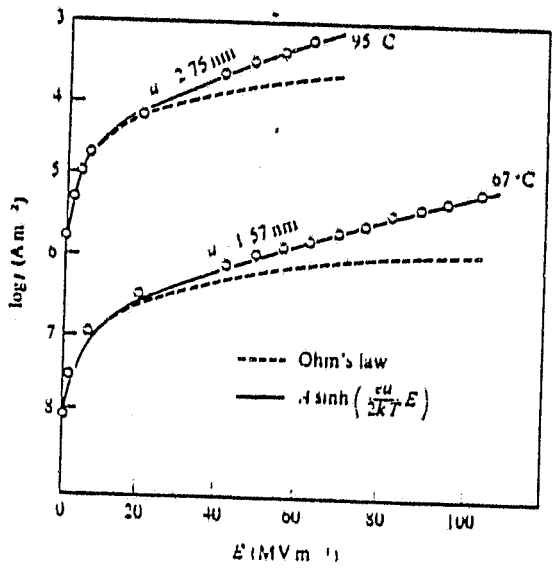

Figure 19 Graphs showing the effect of electric field strength on conduction.

is an applied electric field, K is the Boltzmann constant, and the constant A contains the information for the vibrational attempt frequency as well as the concentration of the ions.

Figure 19 shows the fit of the data of Kosaki et al. (31) for a sample of poly(vinyl chloride) to the equation for ionic conduction. Notice that for this PVC case the actual conduction at 67 degrees C and 100MV/m is approaching a value ten times greater than the ohmic value which one might have projected from the lower field data. We suggest that the ionic conduction equation may be very useful in projecting conduction losses at high fields (beyond the presently attainable electric field strengths) once the moderate field data for the copolymer have been obtained.

Improvements

Once the conduction of the pyroelectric material is quantified at high electric field for various temperatures it may become apparent that the corresponding Joule losses are unacceptably high. If such turns out to be the case then steps must be taken to improve the resistivity of the pyroelectric material. The most obvious improvements may be those associated with the polymer synthesis. A careful analysis of the chemistry of the synthesis process will surely result in important improvements in the insulating properties of the pyroelectric materials produced.

To date, at least two post-synthesis techniques have been successfully applied to "clean-up" partially the ionic impurities in PVDF. One technique was electrodialysis in pure water (23). Another technique was high temperature vacuum bake out (25). Both techniques have shown at least one order of magnitude increase in the resistivity of the polymer.

EXTRACTOR POWER LOSSES

There are three separable types of losses associated with the solid state power extraction-conditioning system. The first is associated with charge up portions of the thermodynamic cycle, the second corresponds to the discharge (extraction) legs of the cycle and the third relates to conditioning the output for consumption by the load. We will discuss only the first two losses here since the third loss is determined by the requirements of an (as yet) unspecified load.

In order to estimate the extractor power losses we must first describe the electrical energy flows into and out of the pyroelectric material. Figure 20 shows the charge versus voltage plot of the pyroelectric cycle. The charge up portion of the cycle begins during the low voltage cool-down between points 2 and 3. During that portion, an external source must transfer electrical energy to the pyroelectric. The area A in figure 21 is equal to the electrical energy which is delivered to the

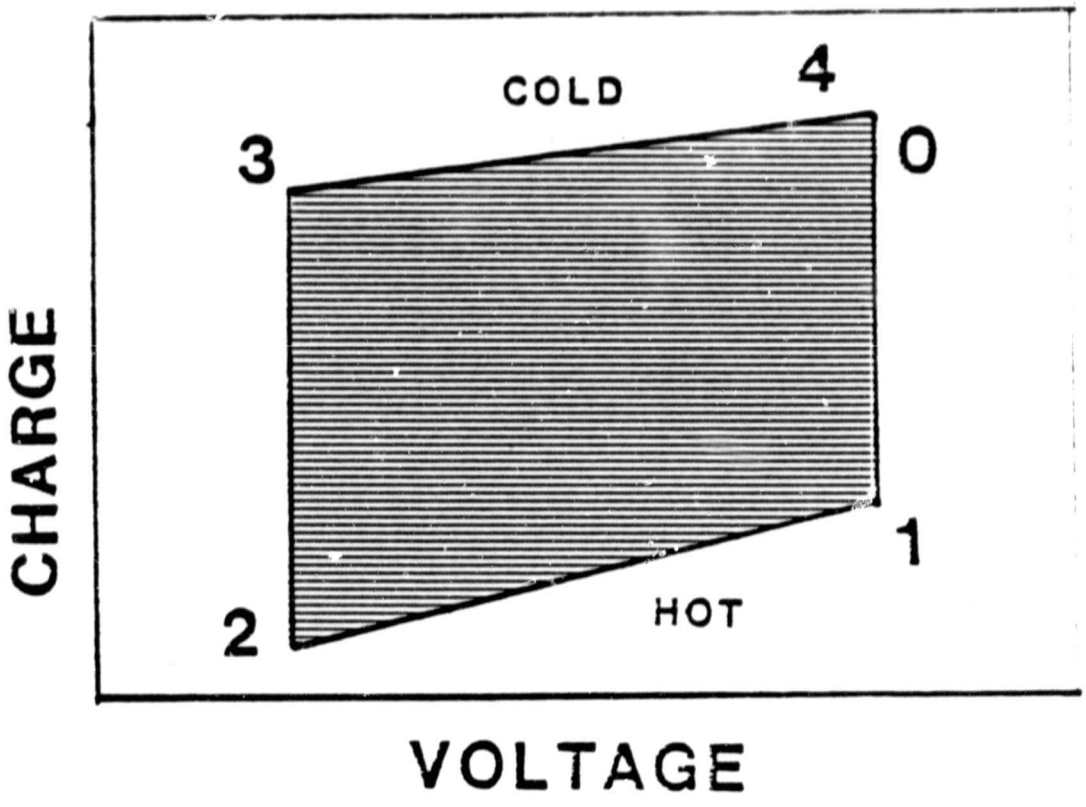

Figure 20 Charge versus voltage plot of a pyroelectric cycle.

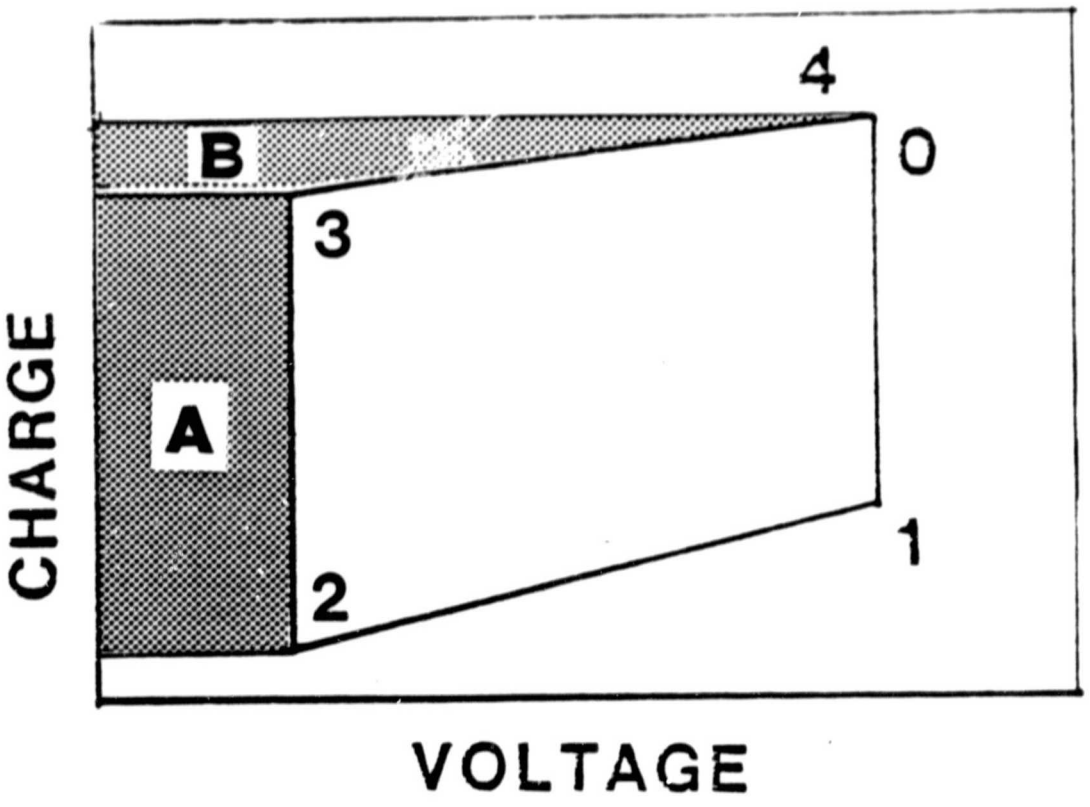

Figure 21 Recharge portions of the cycle.

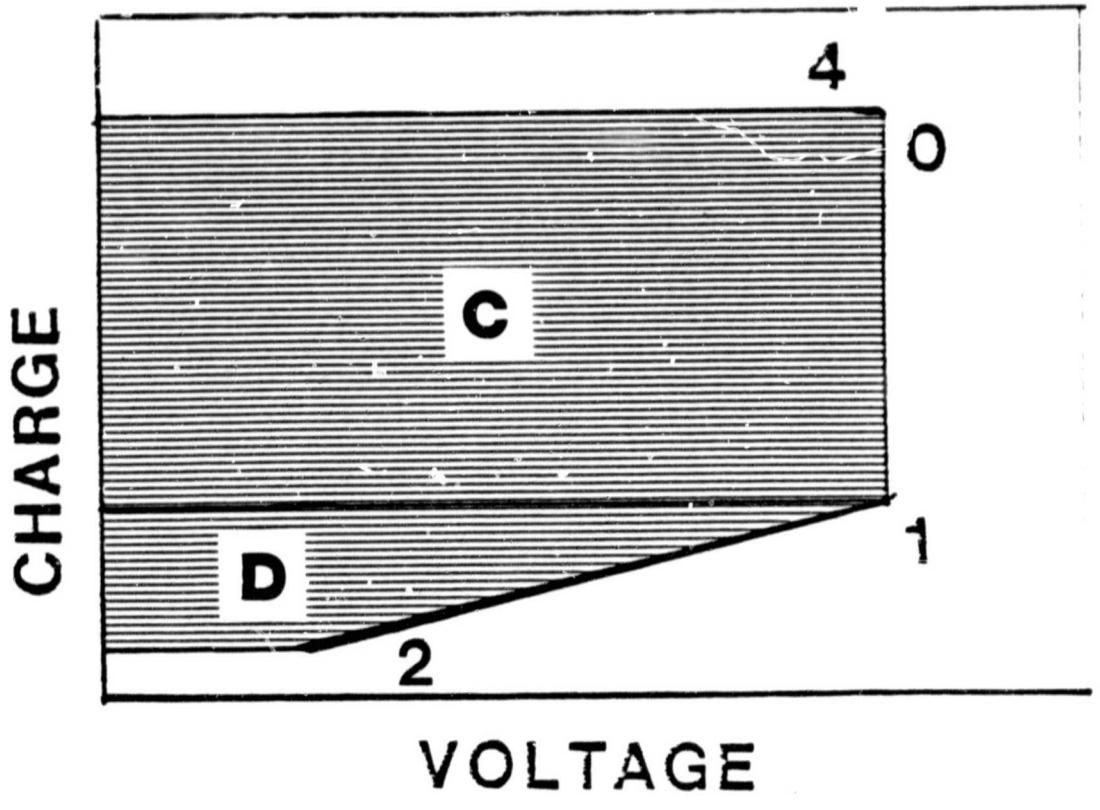

Figure 22 Discharge portions of the cycle.

pyroelectric during the first portion of the charge up. Further charging of the pyroelectric occurs during the cool isothermal voltage ramp-up between points 3 and 4. Once again an external circuit must supply electrical energy, area B, to the pyroelectric. The sum of the electrical energies required to charge-up the pyroelectric, area A plus area B, is loosely analogous to the mechanical compression energy which is necessary in steam turbine cycles.

The electrical energy investment used to charge up the system must necessarily be more than repaid during the remainder of the cycle in order for the pyroelectric converter to be a net producer of electrical energy.

Power output of the pyroelectric begins with the high voltage warm-up which occurs between points 4 (or equivalently 0) and 1. The electrical energy extracted from the pyroelectric to the external circuit is indicated by the area C in figure 22. Additional energy is extracted from the pyroelectric to the external circuit in the hot isothermal voltage reduction from point 1 to point 2 and the energy transferred is represented by the area D in figure 22. The electrical energy output from the pyroelectric during the discharge is equal to areas C plus D. The net electrical output of the cycle is the difference of the discharge energy (area C and D figure 22) minus the charge up energy (area A and B figure 21). The discharge energy exceeds the charge up energy because a portion of the thermal energy which entered the pyroelectric material during the high voltage warm up leg was converted to electrical energy. The net energy of the process is the area shaded in figure 20 (which is identically the same area as had been described earlier when the cycle was first introduced).

What have we gained from this detailed description? First, the electrical energy flows, into and out from the pyroelectric material, have been explicitly shown. Second, we may now more easily describe the electrical circuit losses associated with the injection and extraction of the electrical energy to and from the pyroelectric. As described earlier, the charge transfers may be accomplished with an efficiency of 95% or greater by utilization of switched-mode power supply techniques. The energy loss then may be approximated as 5% of the energy which is circulated into and out of the pyroelectric material during the cycle. If the eventual cycle obtained has the appearance of the cycle in figure 4 then the total injection and extraction loss will be about 10% compared with the net output energy. Measurements of pyroelectric materials under actual power production conditions must be obtained, however, before the number can be refined.

POINTING SYSTEM POWER REQUIREMENTS

Some power will undoubtedly be required in order to maintain the pyroelectric converter pointed toward the Sun and properly oriented with respect to the Earth. Two techniques for maintaining the spacecraft orientation which appear attractive are electric propulsion and controllable solar reflecting panels mounted on long arms. The magnitudes of the powers required appear to be small (less than one percent of the output power) but should be studied further.

Section 4

PERFORMANCE

ENERGY DENSITY

Recent measurements of the charge versus applied voltage (hysteresis) loops of the pyroelectric copolymer have been made at Chronos in collaboration with Dr. J. C. Hicks of the Naval Ocean System Center (NOSC). Preliminary results yield a displacement maximum of about 3 microcoulombs per square cm (30 millicoulombs per square meter) at an electric field maximum of about 500 kv per cm (50 megavolt per meter).

Sample preparation methods limit the dielectric strength and, indirectly, the maximum displacement (the hysteresis loops are not in "hard" saturation).

No power production loop (actual power cycle) has been measured yet (the subject of a future experiment) but, the polarization measurements versus temperature indicate that about 0.5 Joule per cubic centimeter-cycle (0.5 megaJoule per cubic meter-cycle) of electrical energy should be obtainable (high temperature of 100C and a low temperature of 40C) even under the present electric field limitations.

The output energy density is observed to be approximately a linear function of the temperature swing within the temperature band between 40 and 100 degrees Celsius.

If the dielectric strength of this material can be increased to 3.5 MV/cm (350 MV/M), which we have already achieved at 90C with the related homopolymer PVDF, then the energy density will approach 5J/cc-cycle (5 megaJoule per cubic meter-cycle). This value is within the range (2-7 megaJoule per cubic meter-cycle) which we had earlier predicted. The extrapolation to the higher fields is linear in the electric field. Though a high field saturation of the energy density is actually anticipated, an increase in the polarization (displacement) scale is also expected. In the absence of the actual data, we have made the linear estimate.

We caution once again that no power cycles have yet been measured and that the higher dielectric strength copolymer may require substantial effort to obtain.

The crude working approximation for the energy density is;

$$W_e = \text{constant} \times T_s \times E_{max} \qquad (8)$$

where T_s = the temperature swing, E_{max} = the maximum electric

field and the constant is 2.4 E-4 ($J^{-1} V^{-1} K^{-1} M^{-2}$).

DIELECTRIC STRENGTH

Current Value

The present limit of the dielectric strength of the copolymer is about 500 kv/cm (50 megavolt per meter) by our measurements. Yamada (32) has achieved about double this value in some of his experiments even at elevated temperatures. The current limitation on the breakdown strength is likely due the crude physical form of the films which we are able to make. Our method of making the film is to press powders of the copolymer in between two hot (200 C) metal platens. This technique is used because the quantity of the copolymer is very limited.

Expected Limit

Contrast the presently low dielectric strength of the copolymer with that of the homopolymer (PVDF). The manufacturers of the homopolymer sheet state that its strength at room temperature is equal to 5 megavolt/cm (500 megavolt/m). We have measured the ferroelectric properties of the homopolymer at temperatures up to 130 degrees Celsius and have subjected the material to electrical fields in excess of 3.5 megavolt/cm at 90C. Under those conditions the homopolymer was found to degrade (as measured by a decrease in the remanent polarization inducible) in several minutes. At somewhat reduced temperatures and voltages (70C and 2.0 megavolt/cm) this degradation was not detected over the course of hours. These observations were made only incidentally in an experiment which was not concerned with the lifetime of the homopolymer.

Why does the homopolymer seem to have about an order of magnitude greater dielectric strength than the copolymer? Most of the answer lies within the physical form of the experimental films and not in the chemical nature of the material. We have applied our crude preparation procedures to powders of the homopolymer and have also seen low dielectric strength (similar to that measured with the copolymer). The lack of strength in the crude preparations is attributed to 1)greater thickness of the film (it is well established that thinner films in general have higher strength), 2)nonuniformity of thickness of the film, and 3)some impurities (including dust particles) are added to the film during its preparation.

The basic advantage that the existing best-to-date homopolymer has over the copolymer is the physical quality of its manufacture. The technique used in the production of large

quantities of the homopolymer is a film blow. This technique results in a biaxial orientation of the polymer within the plane of the film. This orientation improves the polarization maximum for the material in addition to increasing the dielectric strength.

Our present best estimate as to the intrinsic strength of the copolymer is that it should be approximately equal to that of the currently obtainable value for the homopolymer. This number (300 megavolt/m) should not be mistaken for an ultimate limit for pyroelectric polymers, however.

RADIATION EFFECTS

When polymers are subjected to ionizing radiation, whether it be protons, neutrons, electrons, or photons, two main types of reaction occur, crosslinking and degradation (33),(34). At low dosage the polymer structure determines which reaction predominates. Of primary concern for the operation of the pyroelectric converter are the effects of crosslinking. We presently assume that crosslinking will inhibit the rotation of the pyroelectric polymer about the carbon back-bone. If such an inhibition does take place the thermodynamically important phase transition will be disturbed.

In order to get a feel for the orders of magnitude of the parameters involved, consider the commercially important irradiation of polyethylene film. This polymer is irradiated to a level of about 10 megarad to achieve a high degree of crosslinking (so as to improve its thermal stability and tensile strength). One "rad" of radiation is equivalent to the deposition of 100 erg per gram of irradiated material. The 10 megarad level then corresponds to deposition of 100 Joule of energy into a single gram of material (in SI units, 100,000 gray). Even though this level of irradiation is sufficient to alter dramatically the mechanical properties of polyethylene, it has been shown that the heat of melting of this polymer is little affected by this level of irradiation (the heat of fusion is decreased by 10% and the melting point is depressed by 2 C) (35).

Even though fluorocarbon polymers possess outstanding chemical and thermal stability, they are usually classed among the poorest in resistance to radiation. They are considered to undergo degradation exclusively, and this degradation produces corrosive products. If we include materials having some hydrocarbon groups (e.g. the copolymer), however, crosslinking can occur. The radiation dose at which most useful properties are lost ranges from a few megarad for polytetrafluoroethylene (without hydrocarbon groups) to over 100 megarad for hexafluoropropylene-vinylidene fluoride copolymers (with hydrocarbon groups) (36).

We will next compare this irradiation to that which a polymer is expected to experience in the near earth environment.

The dose rate is given by,

$$\text{Dose(rad)} = 1.6\times10^{-8}\ \text{dE/dx(MeV-cm}^2\text{/gm)} \times \Phi\ \text{(N/cm}^2\text{)} \qquad (9)$$

where dE/dx is the stopping power in the material and Φ is the number of particles incident upon a square centimeter. The stopping power for electrons is about 3 (at 100 keV), and for protons it is about 50 (at 5 MeV) (37).

The flux and dose rate from cosmic rays is the order of $1/cm^2$ sec and less than 10^{-4} rad/hr (38). It would take ten million years to accumulate 10 megarad from cosmic rays. A greater radiation problem is that associated with solar flares. A large solar flare can produce a flux of energetic protons (>5MeV) of 10^5 /cm-sec-steradian and a dose rate in excess of 100 rad/hr. On a yearly basis, less than 10^{10} protons/cm^2-year (8000 rad/yr) are produced even during the peak of the 11-year solar flare cycle. At this rate, the passage of one thousand years is necessary in order to accumulate a potentially disturbing 10 megarad at GEO.

Drastically higher proton fluxes exist at lower altitudes. At the peak, as many as 10^8 /cm^2-sec (1 meV and greater) protons exist.

Figure 23 shows the estimated lifetime of a pyroelectric sheet as a function of altitude. The estimate is based upon the assumption that the life of a pyroelectric sheet will be terminated after the sheet has received 100 megarads of radiation (this is a conservative estimate according to the data of Wang (39). The data for the radiation levels was taken from the Solar Cell Radiation Handbook (37) for zero degree inclination (the worst case) circular orbits. The proton fluences given in the handbook are reported in terms of 1 MeV electron equivalent (for solar cells) fluence. Solar cells are more sensitive to 10 MeV protons than they are to 1 MeV electrons on a per rad basis, and this factor was taken into account when the fluences were converted into rad units.

The solid dots of Figure 23 represent the pyroelectric sheet lifetime as limited by the proton radiation only. The open square symbols indicate the lifetime limitations imposed by both electron and proton radiation. Note that electrons are important only at low altitudes (below 3000 km).

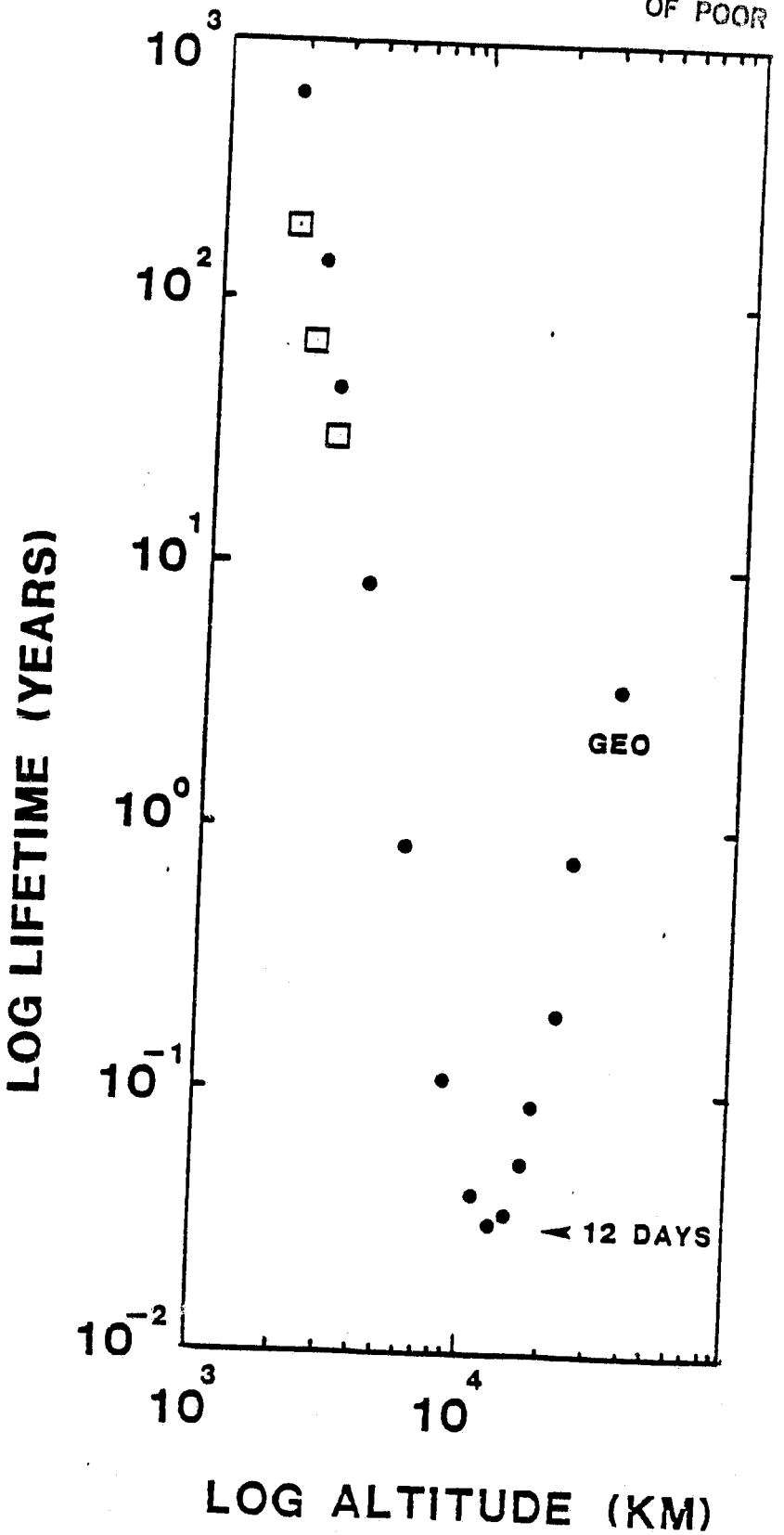

Figure 23 Estimated lifetime of a pyroelectric sheet as a function of altitude.

The lifetimes for the pyroelectric sheet are in the range of 1 to 100 years for all but the most severe region of the Van Allen belt. At the peak radiation levels of the belt, the lifetime of the pyroelectric sheet dips to 12 days. By comparison, an unprotected solar cell would have its output power cut in half in about 0.1 day at that same altitude.

In light of these findings it appears that more detailed knowledge about the effects of radiation on the copolymer - and other pyroelectric polymers - should be obtained.

ELECTRODES

An important question about this large area device is: what will happen if/when a small region of the pyroelectric sheet fails electrically? This is a crucial question since several square meters of sheet will be electrically in parallel within a given segment, and if one region fails as a short circuit then the entire segment may be self shunted. Such localized failure will certainly occur as dielectric breakdown of the plastic may be caused by small voids (from the manufacturing process), pinholes, micrometeoroid punctures, or ionizing radiation damage.

The solution of this potential problem is the incorporation of a technique which assures that point electrical failures result in local open circuiting rather than short circuiting. Researchers interested in studying the properties of various electroactive polymers have already dealt with this problem. They have solved this problem by using thin metallic (vapor deposited) electrodes on their test samples. When a polymer sample with thin electrodes (500 to 1000 Angstrom) suffers a localized dielectric failure the current which pours through the "short" vaporizes the electrode in that region.

It is possible that the self-healing approach may be satisfactory for small areas (a few square centimeters) only. If this turns out to be the case, then it may be be necessary to incorporate some pattern of subdivision with the electroding of each segment. The subdivided electrode patches might be connected by narrow strips of conductor. The entire pattern would be applied in a single plating process with a grid-like mask defining the boundaries between patches. The boundary lines should be kept small so as to minimize arcing from the insulator to the plasma.

The electrodes should be black. The primary purpose for this is, of course, to maximize the radiative heat transfer rates. A secondary benefit of this surface preparation is that it minimizes the optical radiation which actually reaches the pyroelectric material bulk. Though the metallic electrode itself intercepts much of the incident light, a few hundred Angstrom electrode does have a finite transmittance.

Two possible methods of blackening the electrodes are 1)anodization, and 2)coating with carbon. Presently, the second method is preferred since it results in a conducting outer surface which is helpful in minimizing arcing. Other coatings are also possible (40).

EFFICIENCY

The efficiency of the pyroelectric converter may be approximated by the following equation.

$$\text{efficiency} = \frac{W_e - W_{losses}}{C_s T + Q_t} \times R \times E \qquad (10)$$

where W_e is the electrical energy output (density), W_{losses} is the sum of the several energy losses and includes the plasma loss, the bulk conduction loss, and the hysteresis loss, C is the volumetric heat capacity, T is the temperature swing, the product $C_s T$ is called the normal lattice heat, Q_t is the transition heat corresponding loosely to the thermal energy difference between the paraelectric and the ferroelectric phases,R is the efficiency of the thermal radiation cycling (and reflects the heat loss, due to reradiation, during the heat-up of the pyroelectric), and E is the efficiency of the power extractor circuit.

With the following values of the parameters the efficiency may be estimated.

$W_e = 6 \times 10^6 \ J/m^3$ (see Eqn. (8))

$W_{losses} = 23\%$ of W_e

hysteresis loss = 10%

plasma conduction loss = 3%

bulk conduction loss = 10%

$C = 3 \times 10^6 \ J/m^3 K$ (C is actally a function of T and E but the important residuals of that dependence are included in the Q_t term)

T_s = 50 K (thus the normal lattice heat is 1.5×10^8 J/m^3)

Q_t = (the Carnot limit of this heat) = $(12.5\%)^{-1} \times W_e$

$= 4.8 \times 10^7$ J/m^3 (for a thermodynamically ideal cycle, with lattice heat equal to zero, the transition heat is determined by the Carnot limit on the efficiency)

R = 0.85 for the CS-2 design

and finally,

E = 0.90

With this selection of parameters the net system pyroelectric conversion efficiency is estimated to be 2 percent which is about one sixth of the Carnot limit. The principle culprit for the low efficiency is the large value for the lattice heat. The lattice heat may in principle be removed for terrestrial pyroelectric converters by means of heat regeneration. Regeneration is not included in the present design of an extended space pyroelectric converter so the only avenues for system efficiency improvement are 1)reduction of the system losses and 2)increases in the output electrical energy density. Though system improvements seem likely as compared with the conservatively estimated parameters, the greatest improvements are expected with regard to the output characteristics of the present and potential pyroelectric materials.

With a ten fold increase in the output energy density the efficiency of the pyroelectric converter would become 8%. The efficiency scales sublinearly with the increase in the output energy density in this case, because the transition heat of equation (10) also increases with the output energy density. The sources of such an improvement in the output energy density are crystallinity enhancement (current material is 50% crystalline), crystal orientation (present material is not even uniaxially oriented), increased dielectric strength (a byproduct of improved dielectric strength is that the polarization is increased), and new pyroelectric materials.

POWER TO MASS

We will discuss the power to mass in three different ways. In each succeeding manner, more of the system will be included in the power to mass accounting. In the first case only the pyroelectric sheet and its immediate supporting structure will be considered. In the subsequent cases collector mass and, finally, power extractor mass will be included.

The power to mass parameters for the pyroelectric sheet and supporting structure are given in Table I. The assumed values for the energy density and efficiency were explained in the previous subsections. The two columns correspond to the estimated near term performance (in the left column) and a reasonable estimate of performance potentially attainable in the future (shown in the right column). The values in the table are based upon the assumption that the pyroelectric sheet is 10 micrometer thick. The mass per unit area is obtained by assuming a pyroelectric sheet density of 2 and that the supporting structure mass is equal to the pyroelectric sheet mass. This is in keeping with a design rule of thumb which is attributed to Hedgepeth et al. (41). The electrical energy per cycle and electrical power per unit area follow from the information given earlier in the table.

The final entries in Table I show the very large output power per unit mass which is estimated when only the pyroelectric sheet and its immediate supporting structure are included.

Table I Power to mass parameters for the pyroelectric sheet and supporting structure only.

Energy Density (J/m^3)	6×10^6	60×10^6
Efficiency		
Cylinder	1.2%	4.7%
CS-2	2%	8%
Volume per unit area (m^3/m^2)	10^{-5}	10^{-5}
Mass per unit area (Kg/m^2)	0.02 sheet 0.02 support	0.02 sheet 0.02 support
Electrical energy per unit area (J/m^2)	60	600
Electrical power per unit area $(watt/m^2)$		
Cylinder	5	19
CS-2	31	132
Electrical power per unit mass (watt/Kg)		
Cylinder	125	475
CS-2	775	3300

Table II shows the parameters corresponding to a power to mass computation which includes the collector. The heat power required for each of the configurations of Table I is found by dividing the electrical power by the efficiency. The corresponding collector area falls out by assuming an incident solar flux of 1.4 kilowatt per square meter and an optical collection efficiency of about 70 percent. The mass of the collector assumes a collector area density in the range between 12 gm per square meter (41) and 200 gm per square meter (42).

The inclusion of the collector mass brings the near term power to mass ratios for the two designs to within a factor of two of each other. The near term power densities are quite high at about 100 watt per kilogram. These near term estimates compare favorably against the advanced thin blanket photovoltaics which promise 265 watt per kilogram (43). The improved pyroelectric material designs are still more attractive at 400 to 2500 watt per kilogram.

Table II Power to mass including collectors

Heat power required for each of the configurations per unit area of pyroelectric sheet ($watt\ thermal/m^2$)		
Cylinder	414	414
CS-2	1530	1650
Collector area per unit pyroelectric sheet area		
Cylinder	0	0
CS-2	1.18	1.27
Added mass per unit pyroelectric sheet area (Kg/m^2)		
Cylinder	0	0
CS-2	0.24	0.013 to 0.26
Electrical power to mass - including collectors (watt/kg)		
Cylinder	125	475
CS-2	71	440 to 2500

Table III concerns the power to mass ratio with the addition of the power extractor electronics. The power extractor mass per unit electrical output shows a range of values. At the lower end is a conservative rough estimate for the extractor described earlier. At the high end is an accepted mass density for low voltage space power systems (44). Included in the second

row of the table is the mass of the radiator which is required to reject the heat dissipated in the extractor electronics. The assumed area density is taken from Schubert (44).

The final set of entries in Table III gives the electrical power per unit mass for the entire system including the pyroelectric sheet and its supporting structure, the collectors, and the power extraction electronics and associated radiator. The importance of the mass of the extraction electronics to the system is evidenced by a decrease in the power to mass as compared to Table II. An important consequence of this is that the "improved material" design shows less of an enhancement in performance over the near term design. On a total system power to mass basis, however, the pyroelectric system appears more attractive than photovoltaics since solar cells will also require power conditioning (of equal or greater mass per watt).

Table III Power to mass including collectors and power extractors

Power Extractor mass per unit electrical power (90% efficiency) (Kg/watt electrical)	0.001 to 0.0022	0.001 to 0.0022
Power extractor radiator mass per unit electrical power (Kg/watt electrical)	0.0005	0.0005
Electrical power per unit mass including collectors, extractor, and extractor radiator (watt/Kg)		
Cylinder	100	210 to 280
CS-2	62	200 to 530

COST ESTIMATES

The task of estimating costs for a future spacecraft is indeed a tricky one. I have studied the space power literature and found quite a bit of "apples versus oranges" comparisons. One finds quite a number of estimates which are overly optimistic or which do not include important system elements. Often times these stripped down estimates are compared with more complete systems estimates of a competitive approach to show that the competitor is "inferior." I have tried to avoid these pitfalls as much as possible.

Tables IV through VIII show break-downs of the estimated costs for the various components of pyroelectric generator systems. The first two tables correspond to the CS-2 design (at assumed efficiencies of 2% and 8% respectively). The third and fourth tables correspond to the simple cylinder design.

In Table IV the polymer cost is estimated to be about $160 per kilogram. This estimate includes the fact that the current price for 9 micron thick PVDF sheet (biaxially oriented) is $100 per kilogram. In addition it is estimated that the synthesis of the copolymer will be about 60 dollars per kilogram more expensive than the homopolymer. The cost of the support structure is taken as $600 per square meter (42). The metallized concentrator/collector is estimated in this table to cost $1200 per square meter. The higher per area cost of the concentrator corresponds to the greater complexity of the curves required for a collector of concentration ratio equal to 20 (42). The mass for the concentrator is also taken from French (42) in this case and has the value of 0.2 kg per square meter. This is a more conservative assumption as compared with the area mass density of 0.012 kg per square meter for the concentrators of Hedgepeth (41).

Table IV Estimated Cost Components for Pyroelectric Converters Per Kilowatt of Electrical Output (Assuming CS-2 design, efficiency=2%, 6 megajoule per cubic meter electrical output)

Item	$	Area (m^2)	Mass (kg)
Polymer sheet	96	32	0.64
Electroding	640	64	0.32
Support structure	19000	32	0.64
Metallized Collector and structure	46000	38	7.6
Electronics	30000		2
Radiator for Electronics	500	0.1	0.25
Totals	96000		11

Electrical power handling costs are listed under the heading of electronics and are based on the figure of $30 per watt (45). The mass for the power conditioner is assumed to be 2 kg per kilowatt (44). The numbers for the radiator (for the rejection of the heat generated by the power handling electronics) are based upon an assumed extractor efficiency of 90%.Corresponding toeac kilowatt of electric output there will be 100 watts dissipated in the extractor circuits. In order to radiate this 100 watts at 50 degrees Celsius will require 0.1 square meter of 2.5 kg per square meter radiator. The estimated cost for a heat pipe radiator is $5000 per square meter (42).

The costs before power conditioning, for the assumptions of Table IV, total about $96,000 per kilowatt. This may be compared with the estimate of $20,000 to $100,000 per kilowatt for large photovoltaic systems without power conditioning (42). Power conditioning costs for the photovoltaic system will be at least equal to the costs for a pyroelectric system. The mass associated with the photovoltaic system's power conditioning will likely be double that for the pyroelectric system due to the low voltage nature of the photovoltaics ("high current means lots of copper").

Notice that the estimated cost of the pyroelectric sheet material is a trivial $96 per kilowatt. This number is only representative of the basic sheet cost and does not include the

costs of quality assurance inspections and tests, nor does it include overhead costs. However, the higher costs estimated for the electroding and support structure should cover these additional expense.

In order to put the previously mentioned costs in perspective, current space photovoltaic "sheets" cost $100,000 per square meter (46) which is $500,000 per kilowatt.

Table V lists cost estimates in a more optimistic way. Here the pyroelectric conversion efficiency is assumed to be 8% and the electrical output energy density is assumed to be 60 megajoule per cubic meter. Since the energy density has increased by a factor of ten over that of Table IV the costs listed in Table V for the sheet, electroding, and sheet support structure all are seen to drop. Due to the higher assumed efficiency the area and cost of the collector drop by a factor of four. The collector mass also drops relative to that listed in Table IV by at least a factor of four. The mass of the collector may be still twenty fold lighter if a density of 0.012 kg per square meter (41) is achieved.

Table V Estimated Cost Components for Pyroelectric Converters Per Kilowatt of Electrical Output (Assuming CS-2 design, efficiency=8%, 60 megajoule per cubic meter electrical output)

Item	$	Area (m^2)	Mass (kg)
Polymer sheet	23	7.6	0.15
Electroding	150	15	0.07
Support structure	4500	7.6	0.15
Metallized Collector and structure	12000	9.7	0.1 to 2
Electronics	1000		1
Radiator for Electronics	500	0.1	0.25
Totals	18000		1.7 to 3.6

With the assumptions of Table V the cost for the pyroelectric generator (w/o power conditioning) totals $17,000 which is less than the cost of the lower limit for the photovoltaic approach.

The estimates for the mass and cost of the electronics are also listed in a more optimistic tone in Table V (relative to Table IV). The lighter power conditioning corresponds to an advanced design which operates at higher frequencies than are currently common. The reduced power conditioning cost of $1,000 per kilowatt is still much larger than the terrestrial cost of about $100 per kilowatt (47).

Tables VI and VII are similar to Tables IV and V, respectively, where the system which is analyzed is now the simple cylinder design instead of the CS-2 design. The collector costs and masses are eliminated in these cases. This results in systems which are fairly cost competitive with the CS-2 designs. Thus the cylindrical approach still deserves consideration in spite of its larger pyroelectric components. Certainly a judgement as to cost differential between the two pyroelectric designs cannot be drawn from Tables IV through VII as the expected errors in the estimates are larger than the cost differences.

Table VI Estimated Cost Components for Pyroelectric Converters Per Kilowatt of Electrical Output (Assuming cylinder design, efficiency 1.2%, 6 megajoule per cubic meter electrical output)

Item	$	Area (m^2)	Mass (kg)
Polymer sheet	650	200	4
Electroding	4000	400	2
Support structure	120000	200	4
Metallized Collector and structure	0	0	0
Electronics	30000		2
Radiator for Electronics	500	0.1	0.25
Totals	155000		12

Table VII Estimated Cost Components for Pyroelectric Converters Per Kilowatt of Electrical Output (Assuming cylinder design, efficiency=4.7%, 60 megajoule percubic meter electrical output)

Item	$	Area (m^2)	Mass (kg)
Polymer sheet	150	53	1.1
Electroding	1050	106	0.5
Support structure	32000	53	1.1
Metallized Collector and structure	0	0	0
Electronics	1000		1
Radiator for Electronics	500	0.1	0.25
Totals	35000		4

Transportation costs must also be considered. The current shuttle cost (to LEO) is $340 per kilogram (48). For the pyroelectric power systems, with their super light weight, this transportation cost is small (less than 4% of the totals listed in the tables).

Transportation to GEO, however, is a different matter. The transportation cost to the higher altitudes cost $5,000 to $20,000 per kilogram (49). The total systems costs and transportation costs are listed in Table VIII.

Table VIII System and Transportation (to GEO) Cost in Dollars

System cost	Transportation cost
(Assuming CS-2 design, efficiency=2%, 6 megajouleper cubic meter electrical output)	
96,000	55,000 to 220,000
(Assuming CS-2 design, efficiency=8%, 60 megajoule per cubic meter electrical output)	
18,000	8,500 to 72,000
(Assuming cylinder design, efficiency 1.2%, 6 megajoule per cubic meter electrical output)	
155,000	60,000 to 240,000
(Assuming cylinder design, efficiency=4.7%, 60 megajoule percubic meter electrical output)	
35,000	20,000 to 80,000

For comparison, the cost of transporting an advanced photovoltaic array of power density 250 watt per kilogram (43) (4 kg/kw plus 2 kg for power conditioning) to GEO would be $30,000 to $120,000. Therefore, the pyroelectric conversion approach, in addition to its lower capital cost per kilowatt, has the potential advantage of being a third as expensive to transport to high altitudes.

Section 5

SPECIAL CONSIDERATIONS

RADIATION HARDENED DESIGNS

Radiation hardening of the pyroelectric converter may be feasible by at least two design approaches. The first idea is to surround the pyroelectric disk (in the CS-2 design) with a shield against ionizing radiation (see Figure 24). A pancake shaped "can" made of aluminum sheet 76 micrometer (0.003 inch) thick would decrease the ionizing radiation flux substantially. The lifetime for the pyroelectric converter under the worst case orbit conditions described earlier would be increased from 12 days to 1.5 years by the addition of such a shield. Greater lifetime enhancements would be possible if thicker walled shielding were utilized.

The aluminum can sheet would have a mass of about 410 gram per square meter of pyroelectric sheet. Since the 2% efficient pyroelectric converter would have a power density of 31 watt per square meter, the can sheet mass would be 13 gram per watt (13 kg/kw). For the 8% efficient CS-2 design the area power density should be 132 watt per square meter and, therefore the aluminum sheet mass would be 3.1 kg/kw. As mentioned earlier, a rule of thumb in designing the support for a large surface area is that the structure mass will usually range from 50% to 100% of the mass of the sheet which is to be supported. Assuming the upper limit of this range for the support we find that the masses for the shield and structure come to 26 kg/kw and 6.2 kg/kw for the 2% and the 8% efficient designs respectively. These masses should be compared with the system masses derived earlier. The unshielded system mass (pyroelectric sheet, electroding, pyroelectric sheet support structure, collector, power extraction electronics, and radiator for electronics) for the 2% efficient design was 11 kg/kw. The unshielded system mass for the 8% efficient design was 1.7 to 3.6 kg/kw. For both designs, the added aluminum shield would dominate the system mass. Shielded systems might weigh about three times as much as unshielded systems.

It is interesting to note, however, that the (8% efficient) shielded system's total mass of 6.9 to 9.8 kg/kw is very attractive when compared with the 20 kg/kw (50) to 33 kg/kw (51) for space reactors.

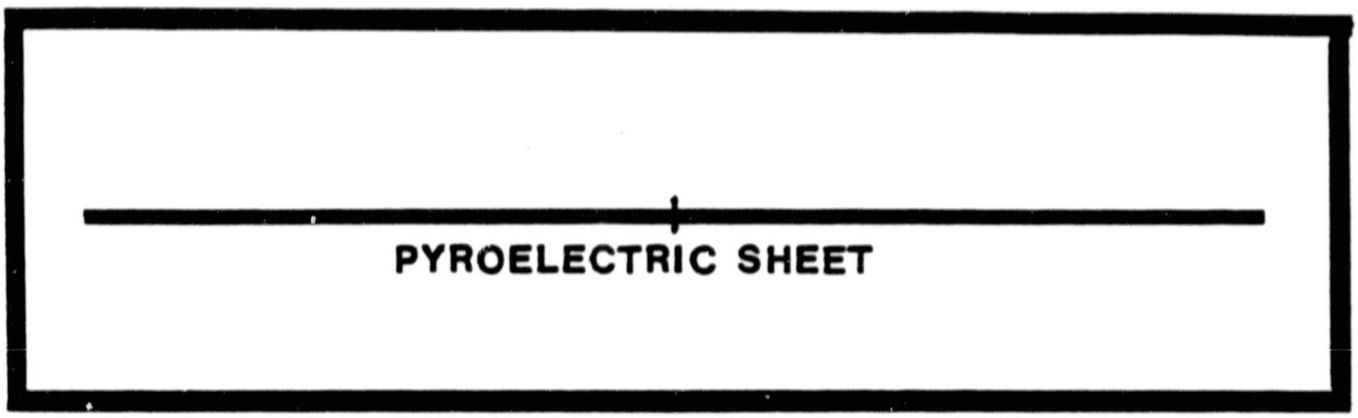

Figure 24 Ionizing radiation shield.

Heat flow for the "can" hardened design

The question immediately arises as to what effect the ionizing radiation shield has upon the thermal radiation. To address this question we wrote a simple computer code, similar to the heat flow calculation described earlier, with the addition of a surface interposed between the pyroelectric sheet and deep space. The interposed surface which represents the aluminum shield is assumed to reach a constant uniform temperature. Since the outward radiating area of the shield is essentially equal to the radiating area of the pyroelectric sheet, the temperature of the shield is determined by the average input power per unit area incident upon the the pyroelectric (incident solar power times concentration ratio times the fraction of the pyroelectric sheet illuminated) and the Stefan-Boltzmann equation. Figure 25, which is similar to Figure 6, illustrates the average temperature and amplitude of the temperature swing of the pyroelectric sheet for the shielded case. The amplitude of the temperature swings is nearly identical to that calculated for the unshielded case. An important difference can be seen in the average temperature. In the shielded case the temperature is higher. For example, the temperature of the shielded pyroelectric sheet is 65 degree higher at a concentration ratio of 8 than would be an unshielded pyroelectric sheet. Thus the ionizing radiation shield also acts as a partial insulator of thermal radiation. Put into different terms, the implementation of a shield necessitates a reduction of about a factor of two in the area power density for the same operating temperature (in the 300 to 600 K range).

The effect of the radiative heat flow considerations is to double the mass per watt of the area dependent components of the pyroelectric system. It may be possible to avoid this penalty, by simply adding a gas (e.g. helium) to the interior of the "can". The convective heat transfer provided by the gas would help to lower the average temperature of the pyroelectric sheet.

A second approach to hardening

Another method for hardening the pyroelectric converter to the effects of ionizing radiation would be to encapsulate the pyroelectric sheet. In this approach the shield is in direct physical contact with the pyroelectric sheet. The most straight forward application of this idea (say placing the aluminum sheets of the previous method in contact with a 10 micrometer thick pyroelectric polymer) would result in a drastic reduction of the efficiency of the converter. The reason this is so is that the added heat capacity of the shield will demand a much greater input of thermal energy than is required to thermally cycle the polymer sheet alone (the reduction in efficiency would be about a factor of 9). If, however, the number of pyroelectric sheets is increased so that the heat capacity of the pyroelectrics dominates over that of the shield, then the efficiency will be little effected.

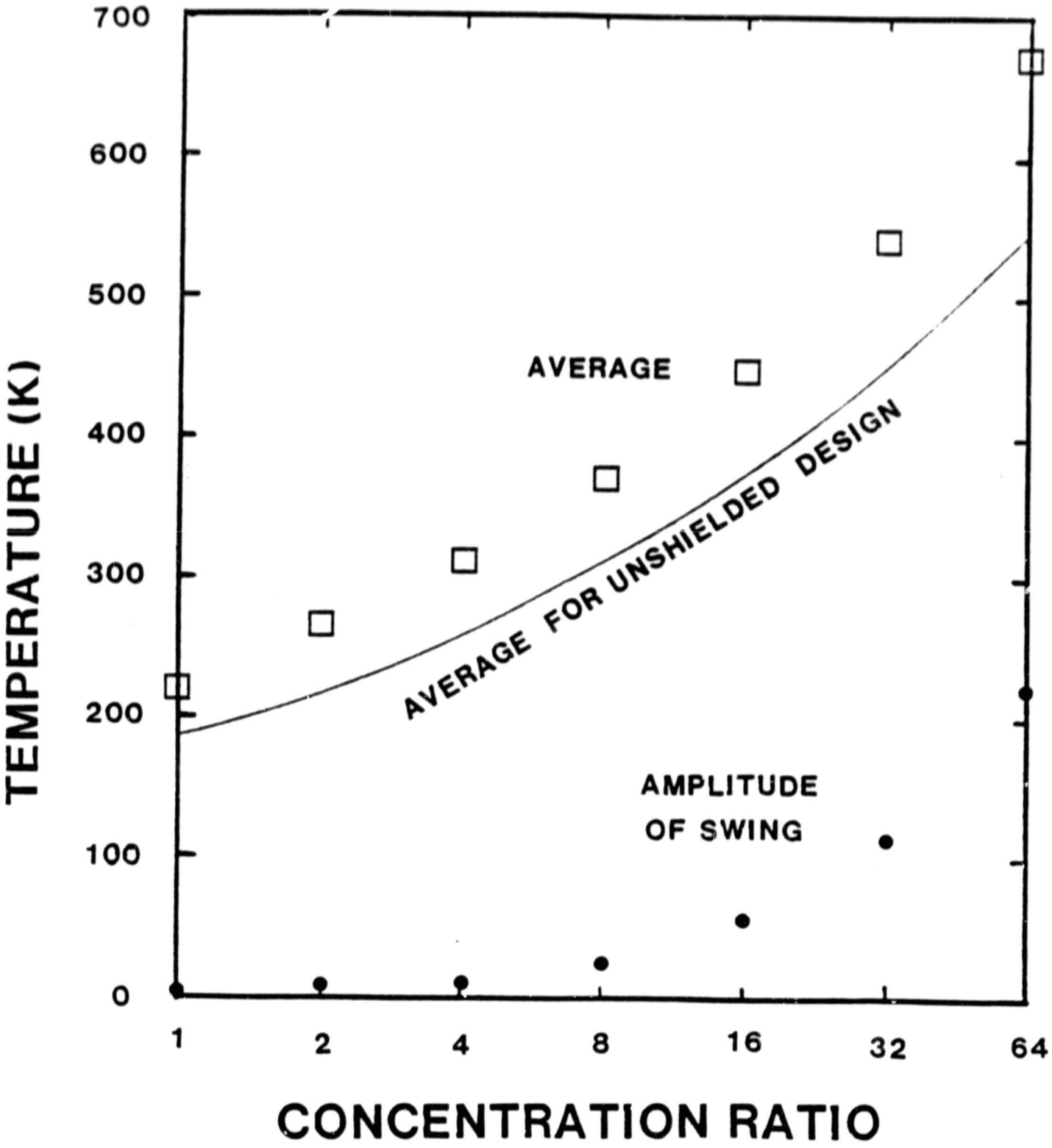

Figure 25 Average temperature for the pyroelectric sheet for the "can" shielded approach.

As an example, assume that the shield material will be the same as the pyroelectric material (so as to minimize thermal expansion mismatch problems). The shields should be of the order of 100 micrometer thick to achieve an attenuation of the ionizing radiation which is comparable to the previously described example. If we require that the thermal loading of the pyroelectric sheet shall not decrease the efficiency by more than 20% then the thickness of the pyroelectrically active material must be at least 1 millimeter (1000 micrometer). The total polymer sheet mass is now 120 larger than our standard 10 micrometer thick sheet. Excluding any consideration for support structure the pyroelectric sheet would have a mass of about 20 kg/kw for a 6.7% (8%/1.2 efficient design. Though support structure considerations might double this calculated mass per unit power, a relaxation of either the efficiency constraint or the amount of shielding constraint, may allow this hardening method to be more competitive.

THERMAL ENERGY STORAGE

Orbiting spacecraft generally require some sort of energy storage. For a satellite which derives its energy from photovoltaics, the energy is stored in the electrical energy of a charged up battery. In a pyroelectric system energy may also be stored in electric batteries. Alternatively, a pyroelectric system may be coupled to a thermal storage element with the partial or complete elimination of electrical batteries.

The energy density of the thermal storage system may exceed that for batteries. Consider the storage of sensible heat in lithium. Lithium's heat capacity is 4 Joule/gm K in the range 973 to 1773 K (52). Over that temperature range, 3200 Joule per gram (3.2 megaJoule per kilogram) of thermal energy may be stored in lithium. If this heat energy is later converted by a 2% efficient pyroelectric device, then the equivalent electrical energy storage is 64 thousand Joule per kilogram (18 W-hr/kg). With an 8% efficient pyroelectric system the equivalent electrical energy density would be 260 thousand Joule per kilogram (70 W-hr/kg). For comparison, the electrical storage energy densities for NiCd and NiH2 batteries are 26 and 40 W-hr/kg (and charging efficiencies of 76% and 65%) respectively (51).

Thermal energy may also be stored by melting a material. The heats of fusion for several materials are given by Severns and Cobble (53) for melting transitions in the range of 1600 to 2100 K. High heats of fusion per kilogram are possible (in the range of one to two megaJoule per kg) and the potential for isothermal heat transfer is attractive. As for any thermal storage which uses a melting medium, heat transfer through the solid phase may present difficulties. In the previous case of the lithium storage material, the lithium remains liquid during the entire thermal cycle.

Figure 26 schematically illustrates a way in which the thermal storage element may be incorporated into a pyroelectric conversion system. Sunlight enters from the top and is concentrated by a Cassegrainian-like mirror system. The thermal storage element sits at the focus of the concentrator. When the spacecraft is in "daylight" the thermal element collects heat while simultaneously delivering heat to the rotating pyroelectric sheet (shown at the bottom of Fig. 26). While the spacecraft is in the sunlight, there is a net gain of heat in the thermal storage element. When the spacecraft passes into the shadow of the earth, aperture "A" is closed to avoid an unnecessary heat loss. The retained heat in the thermal storage element provides continuous radiative heating of the pyroelectric sheet. If the thermal storage medium is of the "sensible heat" type (e.g. lithium), then it will be necessary to open the aperture "B" as the medium cools if constant heat transfer from the medium to the pyroelectric sheet is to be maintained. For the lithium case discussed earlier, the area must change by a factor of eleven. For an isothermal latent heat storage medium, the aperture may remain essentially fixed.

It is well known that the requirement of electrical batteries for an orbiting high power spacecraft has an important impact upon the system mass. Such is also the case for the thermal storage subsystem in a pyroelectric power supply. The mass of batteries (either electrical or thermal) is determined by amount of time that the spacecraft spends in the shadow of the earth. At low orbit the percentage of orbital period spent in the shadow is maximal. At higher orbits the percentage of time spent in the shadow decreases but the amount of time remains fairly constant. For example, the shadow time for a 555 km orbit is 0.59 hour while the shadow times at 5090 and 35800 km are 0.64 and 1.2 hour (for equatorial orbits). Using 0.6 hour of storage and the 18 to 70 W-Hr/kg derived earlier for the thermal storage approach, we may see that 8.6 to 33 kilograms of lithium are required per kilowatt. For comparison the pyroelectric system mass per kilowatt ranged from 2 to 10. Thus thermal storage may be expected to dominate over other component masses in orbiting systems which require large amounts of power when the spacecraft is in the earth's shadow.

The addition of heavy batteries to heavy photovoltaics has (along with compactness and survivablility considerations) led to the apparent attractiveness of the nuclear reactors for 100 kilowatt plus space power systems. It is interesting to note that a pyroelectric system including storage may "weigh in" at about 10 kg per kw. Thus the pyroelectric system may be only half as massive as an advanced reactor system (50).

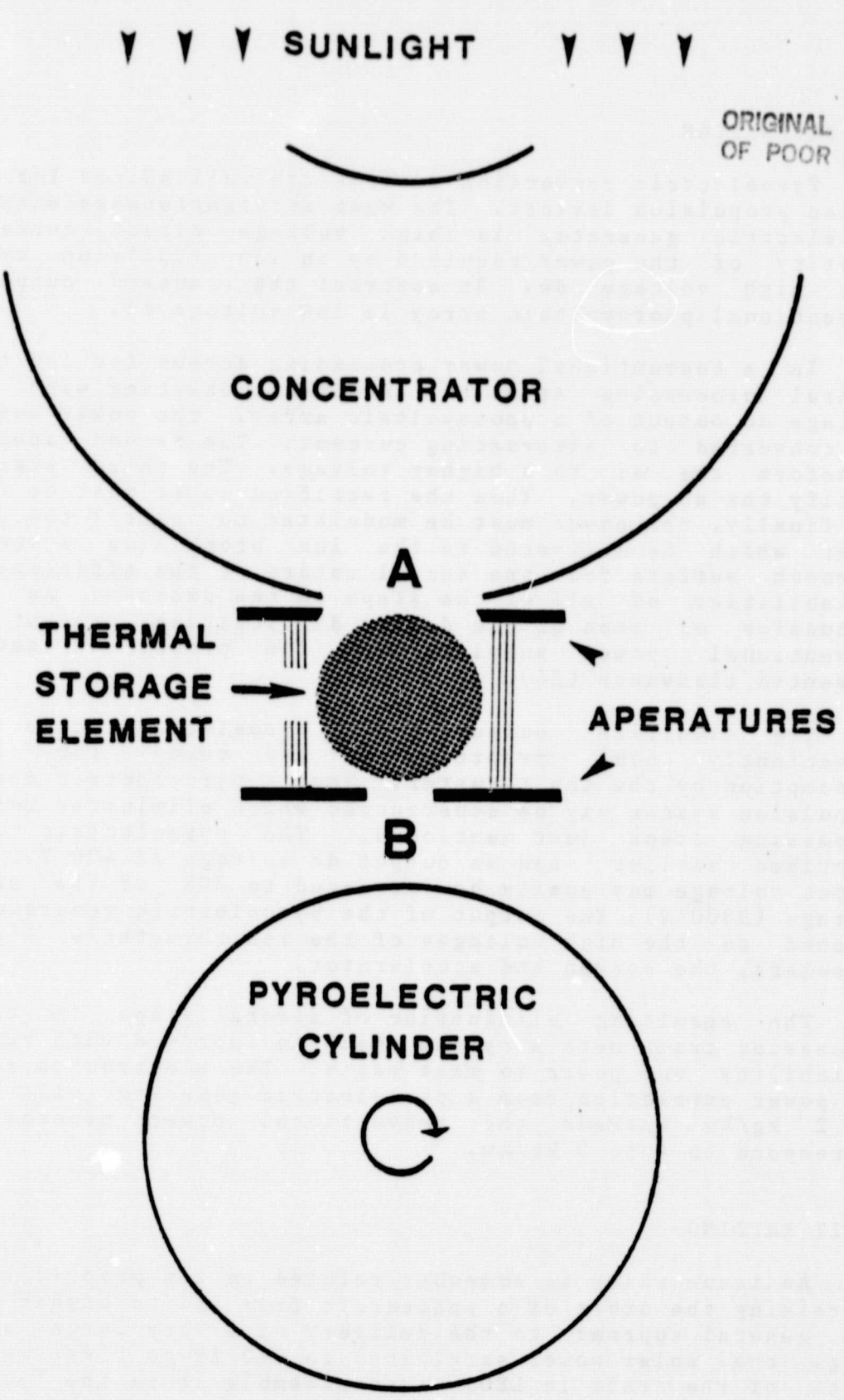

Figure 26 Thermal storage element incorporated in a pyroelectric conversion system.

ION PROPULSION

Pyroelectric conversion systems are well suited for coupling to ion propulsion devices. The most straightforward output of a pyroelectric generator is high voltage direct current. The majority of the power required by an ion propulsion system is also high voltage dc. By contrast the standard output of a conventional photovoltaic array is low voltage dc.

In a conventional power processing scheme for ion thrusters several processing steps are involved. Starting with the low voltage dc output of a photovoltaic array, the power must first be converted to alternating current. The second step is to transform the ac to a higher voltage. The third step is to rectify the ac power. Then the rectified power must be filtered. And finally, the power must be modulated to control the amount of power which is delivered to the ion propulsion system. This approach suffers from the serial nature of the efficiencies and reliabilities of all of the steps in the process. An in-depth discussion of some of the design difficulties present in the conventional power supplies for ion propulsion devices is presented elsewhere (54).

The electrical output of a pyroelectric generator may conveniently come preprocessed and ready for immediate consumption by the ion thruster. Thus a pyroelectric driven ion propulsion system may be constructed which eliminates most of the processing steps just mentioned. The pyroelectric converter described earlier had an output dc voltage of 400 V, but the output voltage may easily be increased to 80% of the extraction voltage (3000 V). The output of the pyroelectric generator may be matched to the high voltages of the ion thruster's high power consumers, the screen and accelerator.

The resulting elimination of several steps in the power processing train nets a system which is improved with respect to reliability and power to mass ratio. The electronics related to the power extraction from a pyroelectric generator will "weigh" 1 to 2 kg/kw whereas the conventional power processing will correspond to 4 to 5 kg/kw.

ORBIT RAISING

An issue which is somewhat related to ion propulsion is that of raising the orbit of a spacecraft from LEO to higher altitude. The general approach to the delivery of a very large spacecraft (e.g. the solar power satellite) to GEO is to first place the parts of the craft in LEO, then assemble it in the "absence of gravity". After assembly the large structure may be transported to GEO by some sort of ferry. Photovoltaic arrays have been suggested as a possible power source for the orbit raising system. Unfortunately, the excursion from LEO to GEO is expected to span several days to several weeks. The extended time spent in the radiation belts would severely damage the photovoltaic cells.

Potentially the pyroelectric converter could be used to power an orbit raising system. Figure 23 shows the estimated lifetime of a pyroelectric sheet as a function of altitude. The lifetimes for the pyroelectric sheet are in the range of 1 to 100 years for all but the most severe region of the Van Allen belt. At the peak radiation levels of the belt, the lifetime of the pyroelectric sheet dips to 12 days. By comparison, an unprotected solar cell would have its output power cut in half in about 0.1 day at that same altitude.

It appears therefore, that pyroelectric converters may have the survivability to provide the power source for orbit raising system. In addition, the pyroelectric systems can dispose of damaged sheets as necessary (at extremely small mass penalty) in order to extend the system lifetime even further.

TECHNOLOGICAL BARRIERS

The technological barriers which stand between the "conception" and the "realization" of pyroelectric conversion in space are naturally numerous. At this early stage we can list only the barriers which are more fundamental. The hurdles seem to fall into four major categories; 1) demonstration of the conversion cycle with the proposed class of polymers, 2) achievement of improved dielectric strength of the material, 3) demonstration of acceptable plasma power losses for low altitude by simulation, and 4) establishment of reasonable lifetime for the pyroelectric material in the harsh environment of space.

Though the type of pyroelectric conversion cycle which we have been discussing has been firmly established for ceramic materials, the experiment to demonstrate the cycle with polymers (in particular the copolymer P(VDF-TrFE)) has yet to be performed. Though the measurements to date on the copolymer (isothermal measurements of electric displacement versus applied electric field at various temperatures) all indicate that this material will indeed be a very good pyroelectric candidate, the actual conversion cycle must be demonstrated. The demonstration will resolve the one remaining question as to the reversibility of the ferroelectric to paraelectric transition under the conditions of the thermodynamic cycle.

The dielectric strength of the copolymer is currently 50 to 100 MV/m. This strength must be improved because it directly effects the amount of electrical energy which may be extracted in a pyroelectric conversion cycle. This issue has been discussed in detail (in the Performance Section). It appears that this problem is solvable.

The plasma power loss issue has also been described earlier. Existing data indicate that the losses at higher altitudes will not be important. At low earth orbit, however, the losses may present a problem since the power losses may be as large as 10%

to 50% of the output of the pyroelectric converter. One must know both the performance of the pyroelectric material and the plasma power loss before the importance of this parasite can be quantified.

The pyroelectric conversion material must be able to operate in the harsh space environment for reasonably long times if it is to fly. The pyroelectric sheet must be able to survive thermal-electrical cycling in a sometimes arcing plasma while energetic particles and x-rays and micrometeoroids are pelting it. Optical degradation will be prevented by the protective nature of the electrodes, but to what extent the polymers can endure the space environment is not yet known. Fortunately, the pyroelectric sheet does not require as long a lifetime as its competitors. The pyroelectric sheet will be lightweight, flexible, and inexpensive. As a result, the pyroelectric sheet may be considered as a consumable. When one sheet wears out it may be ejected (or rolled up and stowed) and easily replaced with a new one.

CONCLUSIONS

This study was very limited in scope and only allows a first order assessment of pyroelectric conversion in space. However, it is apparent that the pyroelectric approach may offer a lighter weight, lower cost alternative to power generation. Potential plasma interactions and radiation degradations do not seem to present any insurmountable difficulties.

Thermal energy storage appears to be feasible and competitive with electrical battery storage. In power generating systems the pyroelectric approach is expected to be substantially lighter than both advanced photovoltaic and reactor technologies. The pyroelectric systems studied will be area intensive, however.

Pyroelectric generators are expected to be resistant to ionizing radiation and be well matched to ion propulsion systems. As a result, this new form of generator may find application in orbit raising missions.

Pyroelectric conversion is attractive and further study is recommended. Near term work should emphasize studies of the conversion cycle, improvements in the dielectric strength of the known pyroelectric polymer, and attempts to discover new candidate materials.

Section 6

REFERENCES

1. Lines, M.E. and Glass, A.M., Principles and Applications of Ferroelectrics and Related Materials, Clarendon, Oxford (1977).

2. Drummond, J. E., "Dielectric power conversion," 10th IECEC, p. 569, (1975).

3. Gonzalo, J. A., "Ferroelectric materials as energy converters," Ferroelectrics 11, 423 (1976).

4. Olsen, R. B., "Ferroelectric conversion of heat to electrical energy--a demonstration," J. Energy, March/April (1982).

5. Olsen, R. B., Briscoe, J. M., Bruno, D. A., and Butler, W. F., "A pyroelectric energy converter which employs regeneration," Ferroelectrics 38, 975 (1981).

6. Olsen, R. B., Briscoe, J. M., and Bruno, D. A., "Performance of a 1-watt pyroelectric converter," 17th IECEC (1982).

7. Beam, B. H., "An exploratory study of thermoelectrostatic power generation for space flight applications," NASA TN-D336 (1960).

8. Beam, B. H., Fry, J. and Russel, L., "Experiments on radiant energy conversion using thin dielectric films," Progress in Astronautics and Aeronautics, Vol. 16, Space Power Systems Engineering, Editors: G. Szego and J. Taylor, Academic Press, 1964.

9. Margosian, P. M., "Parametric study of a thermoelectrostatic generator for space applications," Lewis Research Center, NASA, Cleveland, Ohio, Jan. 4, 1965.

10. Furukawa, T., Date, M., Fukada, E., Tajitsu, Y. and Chiba, A., "Ferroeectric behavior in the copolymer of vinylidene fluoride and trifluoroethylene," Jap. J. Appl. Phys. 19 (1980).

11. Furukawa, T., Johnson, G. E., Bair, H. E., Tajitsu, Y., Chiba, A., and Fukada, E., "Ferroeectric phase transition in a copolymer of vinylidene fluoride and trifluoroethylene," Ferroelectrics 32, 61 (1981).

12. Higashihata, Y., Sako, J. and Yagi, T., "Piezoelectricity of vinylidene fluoride-trifluoroethylene copolymers," Ferroelectrics, 32, 85 (1981).

13. Yamaka, T., Ueda, T. and Kitayama, T., "Ferroelectric-to-paraelectric phase transition of vinylidene fluoride-trifluoroethylene copolymer," J. Appl. Phys. 52, 2 (1981).

14. Yamada, T. and Kitayam, T., "Ferroelectric properties of

vinylidene fluoride-trifluoroethylene copolymers," J. Appl. Phys. 52, 6863 (1981).

15. Middlebrook,R.D.,"Power Electronics: An Emerging Disipline",Proc. IEEE Intern. Symp. Circuits and Systems,(1981).

16. Wildman, P. J. L., "Dynamics of a Rigid Body in the Space Plasma," Progress in Astronautics and Aeronautics, Vol. 71 pp. 633 (1980).

17. McCoy, J.E., Konradi, A., Garriott, O.K., "Current Leakage for Low Altitude Satellites," Progress in Astronautics and Aeronautics", Vol. 71, pp. 523, (1980).

18. Stevens, J.S., "Review of Interactions of Large Space Structures with the Environment," Progress in Astronautics and Aeronautics, Vol. 71 pp. 437 (1980).

19. Freeman, J. W.," Progress in Astronautics and Aeronautics", Vol. 71, pp. 523, (1980).

20. Reiff, P. H., Freeman, J. W., and Cooke, D. L., "Environmental Protection of the Solar Power Satellite," Progress in Astronautics and Aeronautics, Vol. 71 pp. 554 (1980).

21. Purvis, C. K., and Bartlett, R. O., "Active Control of Spacecraft Charging," Progress in Astronautics and Aeronautics, Vol. 71 pp. 299 (1980).

22. Olsen,R.B., Evans, D., Pyroelectric Energy Conversion - Hystersis Loss and Temperature Sensitivity of a Ferroelectric Material, J. Appl. Phys. (1983) in Press.

23. Oka,Y.and Koizumi,N., Effects of Impurity Ions on Electrical Properties of Poly(vinylidene fluoride), Polymer J.,Vol. 14, pp869-876 (1982).

24. Saito,S.,Sasabe,H.,Nakajima,T.,and Yada,K., J. Polym. Sci., A-2,6, 1297 (1968).

25. Olsen,R.B., Hicks,J.C., Broadhurst,M.G., and Davis,G.T., Temperature Dependent Ferroelectric Hysteresis Study of Poly(vinylidene fluoride) submitted to App. Phys. Let. (1983).

26. Sacher,E. Annual Report of Conference on Electrical Insulation and Dielectrical Phenomena, 1980, p 131.

27. Kosaki,M.,Ohshima,H., and Ieda,M., J.Phys. Soc. Jpn., 29, 1012 (1970).

28. Osaki,S.,Uemura,S, and Ishida,Y., J. Polym. Sci.,Polym. Phys. Ed., 9, 585 (1971).

29. Blythe,A.R., "Electrical Properties of Polymers",Cambridge University Press 1979.

30. Mott, N. F., and Gurney, R. W., Electronic Processes in Ionic Crystals, Oxford University Press, (1948).

31. Kosaki,M.,Sugiyama,K., and Ieda,M., J.Appl.Phys.42,3388;31;1598 (1971).

32. Yamada, T. private communication

33. Bovey,F.A."The Effects of Ionizing Radiation on Natural and Synthetic High Polymers," Wiley-Interscience,New York, (1959).

34. Dole,M. editor,"The Radiation Chemistry of Macromolecules,"Vols. 1 and 2, Academic Press, New York, (1973).

35. Salyer,I.O.,et al, Proc. Intersoc. Energy Conv. Eng. Conf. p 948,(1978).

36. Florin,R.E., and Wall,L.A.,"Gamma Irradiation of Fluorocarbon Polymers",J. Res. Nat. Bureau of Stds. Vol.65A,p375, (1960).

37. Tada,H.Y.,et al, Solar Cell Radiation Handbook, 3rd Ed., JPL Publication 82-69, (1982).

38. Vampola,A.L.,Progress in Astro. and Aeron., AIAA, Vol.71, p 339,(1980).

39. Wang,T.T., Ferroelectrics,41,p213-223,(1982).

40. Broadway,N.J. Radiation Effects Design Handbook Section 2. Thermal Control Coatings NASA CR-1786, (1971).

41. Hedgepeth,J.M., Miller,R.K., and Knapp,K., Conceptual Design Studies for Large Free-Flying Solar-Reflector Spacecraft, NASA CR-3438, p 108 (1981).

42. French, E.P., 15th Intersociety Energy Conversion Engineering Conference, p 394 (1980).

43. Rockey, D.E., and Hedgepeth, J.M., "High Performance Solar Arrays Employing Advanced Structures," 16th Intersociety Energy Conversion Engineering Conference, pp.374-379 (1981).

44. Schubert,F.H., Reid,M.A., and Martin,R.E., 16th Intersoc. Ener. Conv. Eng. Conf., p 61 (1981).

45. Mildice, J.W., and Valgora,M.E., 15th Intersociety Energy Conversion Engineering Conference, p 1401 (1980).

46. Scott-Monck, J.A., "Cost and Performance Projections for SPS Photovoltaic Blankets," 16th Intersociety Energy Conversion Engineering Conference, p 255 (1981).

47. Fitzpatrick, G.O., et al., 16th Intersociety Energy Conversion Engineering Conference, p 1962 (1981).

48. Bush, Harold, G., Mikulas, Martin M., and Heard, Walter L., Some Design Considerations for Large Space Structures. Presented at the AIAA/ASME 18th Structrues, Structural Dynamics, and Materials Conference, San Diego, CA, 21-23 March 1977, Paper No. 77-395.

49. Conway, E.J., Walker, G.H., and Heinbockel, J.H., 15th Intersociety Energy Conversion Engineering Conference, p 350 (1980).

50. Mahefkey, T., 16th Intersociety Energy Conversion Engineering Conference, pp 374-379, (1981).

51. Rockey, D.E., Jones, R.M., and Schulman, I., 17th Intersociety Energy Conversion Engineering Conference , pp 70-76, (1982).

52. Douglas, T.B., Epstein, L.G., Dever, J.L., and Howland, W.H., J.Am. Chem. Soc., Vol. 77, p 2144-50, (1955).

53. Severns, J.G., and Cobble, J.H., 16th Interscciety Energy Conversion Engineering Conference , p 89-94, (1981).

54. Sater, B.L., AIAA Paper 73-1103, AIAA 10th Electric Propulsion Conference, (1973).